Article

Discovery of novel celastrol derivatives as Hsp90-Cdc37 interaction disruptors with antitumour activity

Na Li, Manyi Xu, Bing Wang, Zhixian Shi, Zihao Zhao, Yunqing Tang, Xinyue Wang, Jianbo Sun, and Li Chen

J. Med. Chem., **Just Accepted Manuscript** • DOI: 10.1021/acs.jmedchem.9b01290 • Publication Date (Web): 14 Nov 2019

Discovery of novel celastrol derivatives as Hsp90-Cdc37 interaction disruptors with antitumour activity

Na Li[δ], Manyi Xu[δ], Bing Wang, Zhixian Shi, Zihao Zhao, Yunqing Tang, Xinyue Wang, Jianbo Sun*, and Li Chen*

State Key Laboratory of Natural Medicines, Department of Natural Medicinal Chemistry, School of Traditional Chinese Pharmacy, China Pharmaceutical University, 24 Tong Jia Xiang, Nanjing 210009, People's Republic of China

ABSTRACT

To develop novel and efficient heat shock protein 90-cell division cycle 37 (Hsp90-Cdc37) interaction disruptors, several lipophilic fragments were introduced into celastrol (CEL) to synthesize 48 new CEL derivatives. Among all the target compounds, **41** was screened with superior anti-proliferative activity on related cancer cells (IC_{50}: 0.41 ~ 0.94 μM), and **41** could decrease the level of the Hsp90-Cdc37 complex in A549 cells. The capability to disrupt the Hsp90-Cdc37 interaction was stronger than that of CEL. Furthermore, pull-down assay, UV assay and molecular docking analysis all showed that **41** might disrupt the interaction of the Hsp90-Cdc37 complex by preferentially binding to Cdc37 in cancer cells. Further studies showed that **41** could significantly regulate the levels of Hsp90-Cdc37 clients, thereby inducing the apoptosis of cancer cells. Together, **41** is a novel Hsp90-Cdc37 disruptor by binding to Cdc37 (hydrogen bond and/or covalent bond). Our results may provide reference for the discovery of effective Hsp90-Cdc37 disruptors.

INTRODUCTION

Heat shock protein 90 (Hsp90, 90-kDa) is a protein chaperone that is considered as a promising anticancer target.[1] Generally, Hsp90 needs to form a complex with cochaperones to ensure the proper folding and maturation of the client proteins. These cochaperones include cell division cycle 37 (Cdc37), heat shock protein 70 (Hsp70), heat shock protein 40 (Hsp40), homeodomain only protein (Hop), p23, etc.[2] Among them, Cdc37 targets many protein kinases related to the occurrence and development of cancer, such as protein kinase B (Akt), cyclin-dependent kinases 4 (Cdk4), epidermal growth factor receptor (EGFR), human epidermal growth factor receptor-2 (Her-2), and tyrosine-protein kinase Met (c-Met), etc.[3,4] Cdc37 can stabilize the catalytic domains of these kinases, while Hsp90 can maintain their correct conformation.[5] Thus, the functions of these oncogenic kinases depend on the Hsp90-Cdc37 complex. Disruption of on the tHsp90-Cdc37 interaction could regulate the expression of kinases to inhibit the proliferation of cancer cells.[6]

Celastrol (CEL) has been reported to inhibit the proliferation of various tumours *in vitro* and *in vivo*, such as gliomas, hepatocellular carcinomas and prostate cancer.[7-9] The anti-proliferative activity of CEL has been indicated to result from disruption of the interaction between Hsp90 and Cdc37, and this interaction is mainly located at the N-terminal domain of Hsp90 ($Hsp90_N$) and the middle domain of Cdc37 ($Cdc37_M$).[10-12] In the structure of the human $Hsp90_N$-$Cdc37_M$ complex, an important hydrogen bond between Q133 ($Hsp90_N$) and R166/R167 ($Cdc37_M$) was identified as the key interaction for the $Hsp90_N$-$Cdc37_M$.[12] CEL was reported to disrupt this key hydrogen bond due to its location in the hydrophobic pocket.[10,11] However, as a

pentacyclic triterpenoid, the spatial structure of CEL is too large to embed the intersection angle of R166 and R167 in the structure of human Cdc37.[11] In order to disrupt the key hydrogen bond more efficiently, Xu et al recently reported a series of CEL hybrids incorporated with methyl ferulate and its derivatives (hydrophobic structures) and the antiproliferative activity of these hybrids was higher than that of CEL. The immunoprecipitation experiment showed that compound **29** (Xu's study) disrupted the Hsp90-Cdc37 interaction more efficiently than CEL.[13] Thus, introduction of a hydrophobic structure to CEL may be a promising strategy in the discovery of CEL derivatives as Hsp90-Cdc37 interaction disruptors.

To elucidate the structure-activity relationship of CEL derivatives as Hsp90-Cdc37 disruptors and to improve the druglike properties, Jiang's study reported a series of CEL derivatives and found a more potent compound **CEL20**.[14] Compared to CEL, although the solubility of **CEL20** incorporated a polar group was greatly improved (51.2 *vs* 1.44 μg/ml), the Hsp90-Cdc37 disruption activity [IC_{50} (4.71 *vs* 6.49 μM)] was only slightly improved. And the antiproliferative activity of **CEL20** was similar to those of the most compounds incorporated hydrophobic groups [IC_{50} (1.12 *vs* 1.20-1.97 μM]. Moreover, Jiang still emphasized the importance of the hydrophobic interaction and a covalent bond between CEL and Cdc37 in the Hsp90-Cdc37 disruption activity in their design idea. Based on the previous studies, we designed a series of CEL derivatives in which 29-carboxyl group was modified with lipophilic fragments via different linkers and hope that these new compounds disrupted the interaction of the Hsp90-Cdc37 complex by the non-covalent and/or covalent

combination with the target protein.

The structure of cinnamic acid (CA), which consists of a phenyl ring substituted with an acrylic acid, contains highly conjugated π-electron with high hydrophobicity. This structural characteristic allows it to easily bind to hydrophobic pockets.[15,16] Recent studies have reported that CA exhibits potential anti-tumor activity in several cancer cells.[17] In terms of the modification of natural products, CA is widely used to enhance the anti-tumor activity of the parent compounds.[18-20] Thus, CA and its analogues were first introduced to CEL to improve the capability of disrupting the Hsp90-Cdc37 complex and inhibiting cancer cells.

At present, the structural modifications of CEL mainly focus on the C-20 carboxylic acid functionality and alterations of the A, B rings.[21,22] However, many derivatives modified at the A, B rings were unstable.[22-23] These derivatives were oxidized to CEL quickly upon purification, storage and incubation with culture medium.[21] Therefore, considering the stability of the target compounds, CA and its analogues were introduced to the 20-carboxylic acid of CEL by different linkers to afford in a total of 48 new compounds (**1**-**48**). Their anti-proliferative activities were screened *in vitro*. The activity of **41** (IC_{50}: 0.41 ~ 0.94 μM) was comparable with that of bardoxolone methyl (CDDO-Me). Furthermore, the capability of **41** to disrupt the Hsp90-Cdc37 interaction was stronger than that of CEL. In addition, in-depth mechanistic studies of **41** were evaluated to explain the anti-proliferative activity.

RESULTS AND DISCUSSION

Chemistry. The synthetic route of compounds **1**-**48** was shown in Scheme 1.

Trans-cinnamic acid (**1a**) or 4-methylcinnamic acid (**1b**) or 4-methoxycinnamic acid (**1c**) or 4-Fluorocinnamic acid (**1d**) or 4-(trifluoromethyl) cinnamic acid (**1e**) was first treated by the indicated bromohydrins using 1-(3-dimethylaminopropyl)-3-ethylcarbodiimide hydrochloride (EDCI) and dimethylaminopyridine (DMAP) as catalysts in dichloromethane (CH_2Cl_2) at room temperature to get compounds **2f-t**.[24] In a similar way, compounds **6f-t** and **10f-t** were obtained under the treatment of **5a-e** and **9a-e**, respectively. Besides, intermediates **10u-w** were prepared by trans-1,4-dibromo-2-butene in acetone, catalysed by potassium carbonate (K_2CO_3) and tetrabutylammonium bromide ($Bu_4N^+Br^-$) at 50 ^oC.[25] α-cyano substituted cinnamic acids (α-CN CA) **5a-e** were furnished by the condensation of aryl formaldehydes **3a-e** and cyanoacetic acid **4a**, while β-cyano substituted cinnamic acids (β-CN CA) **9a-e** were synthesized by arylacetonitriles **7a-e** and glyoxylic acid **8a** with K_2CO_3 in methanol (MeOH).[24,25] Subsequently, the target compounds **1-48** were accomplished through connecting **2f-t** or **6f-t** or **10f-w** to CEL at C-20 position in the presence of sodium bicarbonate ($NaHCO_3$) in N,N-dimethylformamide (DMF).[13] The substituent groups R^1-R^3 of **1-48** were shown in Table 1.

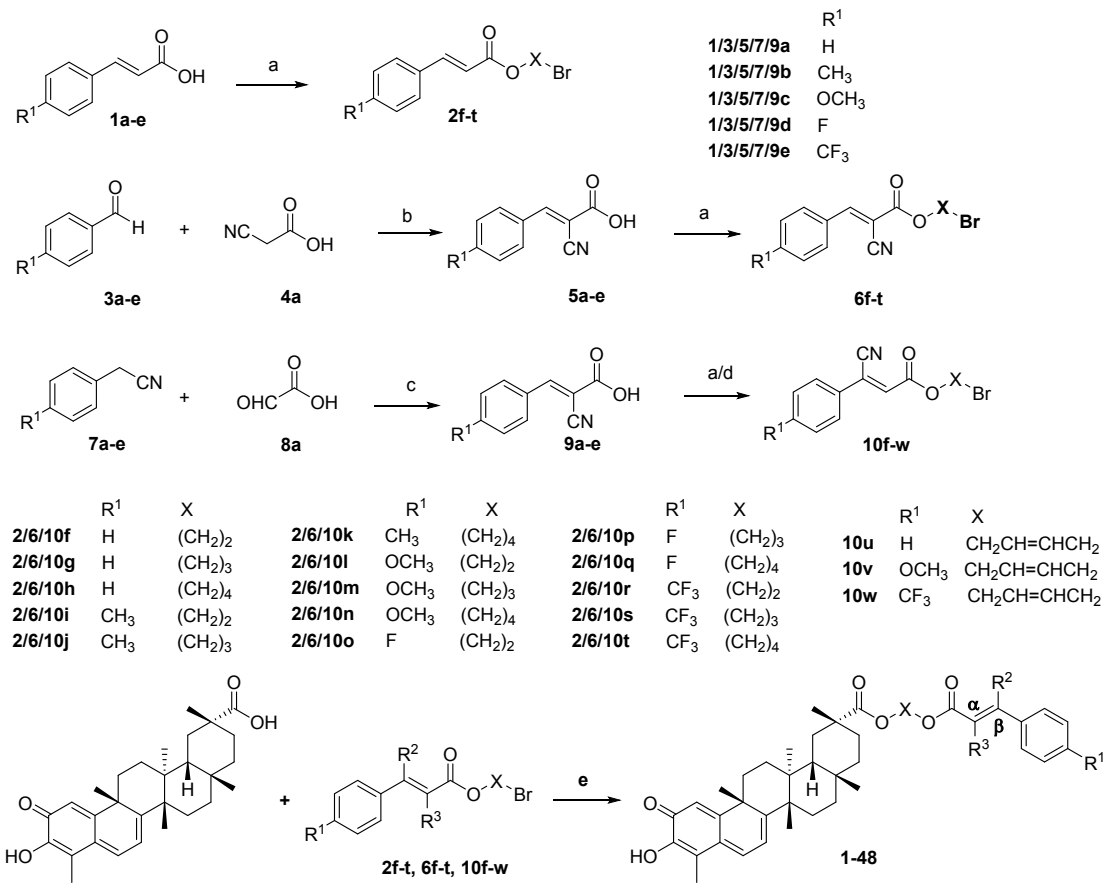

Scheme 1. Reagents and Conditions: (a) various bromohydrin, EDCI, DMAP, CH_2Cl_2, rt, 7 h; (b) NH_4OAc, tolune, 100 °C, reflux, 12 h; (c) CH_3OH, K_2CO_3, 60 °C, reflux, 6 h; (d) bromohydrin, EDCI, DMAP, CH_2Cl_2, rt, 7 h or trans-1,4-dibromo-2-butene, K_2CO_3, $Bu_4N^+Br^-$, acetone, 50 °C, reflux,7 h; (e) celastrol, $NaHCO_3$, DMF, 60 °C, 7 h.

Table 1 The substituent groups (R^1-R^3) of **1-48**.

Cpd.	X	R^1	R^2	R^3	Cpd.	X	R^1	R^2	R^3
1	$(CH_2)_2$	H	H	H	**25**	$(CH_2)_2$	F	H	CN
2	$(CH_2)_3$	H	H	H	**26**	$(CH_2)_3$	F	H	CN
3	$(CH_2)_4$	H	H	H	**27**	$(CH_2)_4$	F	H	CN
4	$(CH_2)_2$	CH_3	H	H	**28**	$(CH_2)_2$	CF_3	H	CN

5	$(CH_2)_3$	CH_3	H	H	**29**	$(CH_2)_3$	CF_3	H	CN
6	$(CH_2)_4$	CH_3	H	H	**30**	$(CH_2)_4$	CF_3	H	CN
7	$(CH_2)_2$	OCH_3	H	H	**31**	$(CH_2)_2$	H	CN	H
8	$(CH_2)_3$	OCH_3	H	H	**32**	$(CH_2)_3$	H	CN	H
9	$(CH_2)_4$	OCH_3	H	H	**33**	$(CH_2)_4$	H	CN	H
10	$(CH_2)_2$	F	H	H	**34**	$(CH_2)_2$	CH_3	CN	H
11	$(CH_2)_3$	F	H	H	**35**	$(CH_2)_3$	CH_3	CN	H
12	$(CH_2)_4$	F	H	H	**36**	$(CH_2)_4$	CH_3	CN	H
13	$(CH_2)_2$	CF_3	H	H	**37**	$(CH_2)_2$	OCH_3	CN	H
14	$(CH_2)_3$	CF_3	H	H	**38**	$(CH_2)_3$	OCH_3	CN	H
15	$(CH_2)_4$	CF_3	H	H	**39**	$(CH_2)_4$	OCH_3	CN	H
16	$(CH_2)_2$	H	H	CN	**40**	$(CH_2)_2$	F	CN	H
17	$(CH_2)_3$	H	H	CN	**41**	$(CH_2)_3$	F	CN	H
18	$(CH_2)_4$	H	H	CN	**42**	$(CH_2)_4$	F	CN	H
19	$(CH_2)_2$	CH_3	H	CN	**43**	$(CH_2)_2$	CF_3	CN	H
20	$(CH_2)_3$	CH_3	H	CN	**44**	$(CH_2)_3$	CF_3	CN	H
21	$(CH_2)_4$	CH_3	H	CN	**45**	$(CH_2)_4$	CF_3	CN	H
22	$(CH_2)_2$	OCH_3	H	CN	**46**	$CH_2CH{=}CHCH_2$	H	CN	H
23	$(CH_2)_3$	OCH_3	H	CN	**47**	$CH_2CH{=}CHCH_2$	OCH_3	CN	H
24	$(CH_2)_4$	OCH_3	H	CN	**48**	$CH_2CH{=}CHCH_2$	F	CN	H

Biological Activity.

In Vitro Anti-proliferative Activity of CEL Derivatives

We first synthesized compounds **1**-**45** with saturated linear alkyl chains as linkers in this study. The inhibition rates of **1**-**45** were determined in A549 cells at concentration of 1.5 μM (Table 2). CEL was used as a positive control. As shown in Figure 1A, the inhibition rates of the CA-CEL hybrids **1**-**15** (blue, 6.19%-37.61%) and α-CN substituted CA-CEL hybrids **16**-**30** (red, 3.07%-34.68%) were lower than that of CEL (purple, 47.98%). These results indicated that the introduction of CA and α-CN-substituted CA decreased the anti-proliferative activities of CEL. Surprisingly, when β-CN-substituted CA was introduced into CEL, the activities of several derivatives increased (green, Figure 1A). For example, the anti-proliferative activities of **31** (59.65%), **32** (53.69%), **37** (48.11%), **38** (53.38%), **40** (65.87%) and **41** (78.45%) were higher than that of CEL (47.98%). In the β-CN-substituted CA-CEL hybrids (**31**-**45,** Figure 1B), the substituent on the benzene ring could affect the activity following the order of F > H > OCH_3 > CF_3 > CH_3. These results indicated that the introduction of an electron-withdrawing group (F, OCH_3 and CF_3) onto the benzene ring might enhance anti-proliferative activity. However, as the presence of electron withdrawing substituent increases, the activity would decrease (F> OCH_3 and CF_3). Furthermore, we found that the length of the linker also significantly regulated the activity (Figure 1D). For example, the inhibition rates of **40** with a 2-carbon linker (65.87%) and **41** with a 3-carbon linker (78.45%) were much higher than that of **42**

with a 4-carbon linker (32.15%). This phenomenon occurred with all target compounds in this study (Figure 1D). These results suggested that once the length of linker reached four carbons, the inhibitory effects were reduced sharply (black arrows) (Figure 1D).

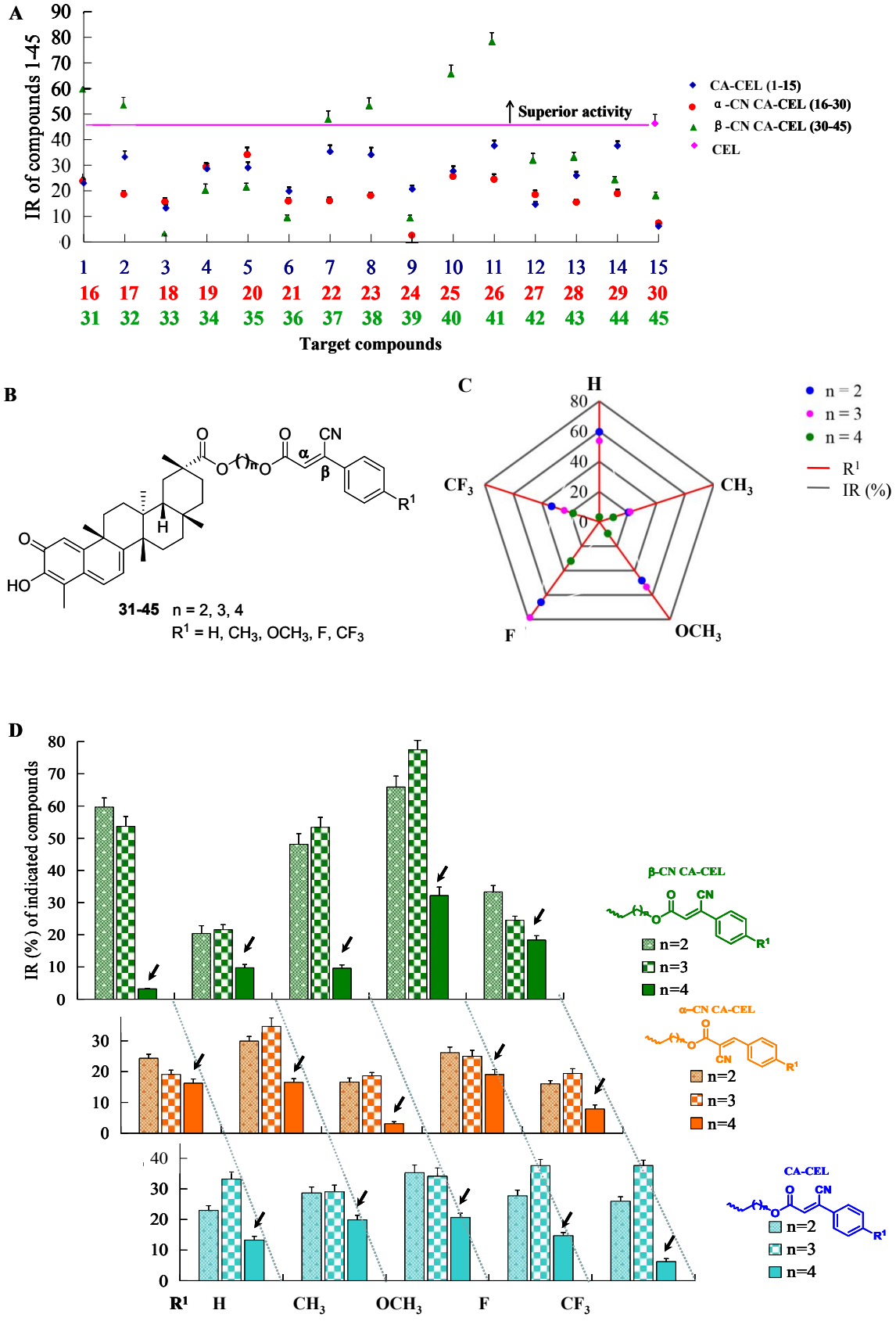

Figure 1. Comparison of inhibition rates of target compounds. (A) Inhibition rates of

1-45 and CEL at 1.5 μM in A549 cells. IR: inhibition rate. (B) The average inhibition rates of **31-45** classified by the different groups in benzene. (C) Inhibition rate of **31-45**. (D) Inhibition rate of **1-45** classified by lengths of linker.

Table 2. Preliminary inhibitory effects of **1-45** and CEL in A549 cells

Cpd.	IR[a]	Cpd.	IR	Cpd.	IR	Cpd.	IR
1	22.97 ± 1.65	**13**	25.97 ± 1.45	**25**	26.15 ± 1.82	**37**	48.11 ± 3.32
2	33.21 ± 2.33	**14**	37.61 ± 1.77	**26**	24.99 ± 1.95	**38**	53.38 ± 3.11
3	13.27 ± 1.25	**15**	6.19 ± 1.02	**27**	19.00 ± 1.67	**39**	9.57 ± 1.08
4	28.65 ± 1.99	**16**	24.29 ± 1.34	**28**	16.03 ± 1.06	**40**	65.87 ± 3.43
5	29.06 ± 2.17	**17**	19.09 ± 1.38	**29**	19.40 ± 1.54	**41**	78.45 ± 3.59
6	19.87 ± 1.52	**18**	16.19 ± 1.43	**30**	7.85 ± 0.34	**42**	32.15 ± 2.67
7	35.32 ± 2.48	**19**	29.87 ± 1.54	**31**	59.65 ± 2.87	**43**	33.30 ± 1.98
8	34.11 ± 2.76	**20**	34.68 ± 2.75	**32**	53.69 ± 3.05	**44**	24.51 ± 1.26
9	20.65 ± 1.39	**21**	16.49 ± 1.22	**33**	3.19 ± 0.12	**45**	18.33 ± 1.38
10	27.74 ± 1.88	**22**	16.59 ± 1.32	**34**	20.40 ± 2.43	CEL[b]	47.98 ± 3.29
11	37.63 ± 2.01	**23**	18.64 ± 1.05	**35**	21.59 ± 1.55		
12	14.71 ± 1.04	**24**	3.07 ± 0.65	**36**	9.74 ± 1.03		

[a] IR: Inhibition rate (%) at 1.5 μM.

[b] Positive control.

According what mentioned above, a F/H/OCH_3 group substituted onto the benzene ring of β-CN-substituted CA-CEL hybrids showed higher activity than that of the CF_3/CH_3 groups. To study the effects of the unsaturated alkyl group on the

anti-proliferative activity, we replaced the linkers of the F/H/OCH_3-substituted β-CN CA-CEL hybrids with unsaturated alkyl chains to obtain **46**, **47** and **48**, respectively. Then, compounds **31**, **32**, **37**, **38**, **40** and **41**, with stronger inhibitory activities than CEL, along with **46-48** were evaluated to determine their IC_{50} values against four tumour cell lines (A549, HOS, MCF-7 and HepG2) with the MTT method (Table 3). As a triterpenoid derivative with multiple-target, CDDO-Me was used as a positive control. As shown in Table 3, the anti-proliferative activities of **46** (IC_{50}: 2.86 ~ 3.54 μM), **47** (IC_{50}: 1.34 ~ 2.71 μM) and **48** (IC_{50}: 1.11 ~ 2.74 μM) had not improved significantly, which suggested that the unsaturated alkyl linker showed little effect on the activity in this study. Among all the compounds, **41**, which showed the highest activity (IC_{50}: 0.41 ~ 0.94 μM) against cancer cells, attracted our attention. Therefore, **41** was selected for further investigation.

Table 3. Anti-proliferative activity of the selected compounds against four cancer cell lines.

Cpd.	IC_{50}			
	A549	MCF-7	HOS	HepG2
31	1.02 ± 0.12	0.70 ± 0.08	0.54 ± 0.05	0.65 ± 0.15
32	1.41 ± 0.17	0.98 ± 0.05	0.45 ± 0.07	0.76 ± 0.13
37	1.79 ± 0.15	0.97 ± 0.09	1.14 ± 0.07	0.97 ± 0.10
38	1.09 ± 0.13	1.10 ± 0.08	1.75 ± 0.05	1.27 ± 0.09
40	1.02 ± 0.15	2.35 ± 0.12	2.18 ± 0.14	3.89 ± 0.28
41	0.41 ± 0.11	0.64 ± 0.07	0.90 ± 0.05	0.94 ± 0.23

46	3.54 ± 0.11	2.86 ± 0.16	4.78 ± 0.19	3.45 ± 0.16
47	1.34 ± 0.14	1.44 ± 0.14	1.79 ± 0.17	2.71 ± 0.18
48	1.84 ± 0.17	1.11 ± 0.13	1.33 ± 0.15	2.74 ± 0.19
CEL	1.48 ± 0.18	2.04 ± 0.15	1.46 ± 0.14	3.18 ± 0.32
CDDO-Me[a]	0.52 ± 0.09	0.85 ± 0.13	0.66 ± 0.11	0.52 ± 0.08

[a] Positive control.

***41** Disrupted the Hsp90-Cdc37 Interaction In Vitro*

Many studies have reported that CEL and its derivatives could disrupt the interaction of Hsp90-Cdc37 interaction. To verify whether **41** decreased the level of the Hsp90-Cdc37 complex *in vitro*, co-immunoprecipitation was carried out in the following experiments. First, we needed to confirm that **41** could not inhibit ATP binding to Hsp90. As shown in Figure 2A, Hsp90α was pulled down by γ-phosphate-linked ATP-sepharose. It has been reported that CEL could not block the ATP-binding pocket of Hsp90. Similar to CEL, **41** had no effect on ATP binding. Next, immunoblot analysis of Cdc37 was carried out after immunoprecipitation of Hsp90α. Compared with the DMSO group, **41** could decrease the amount of Cdc37 detected when Hsp90α was pulled down with **41** treatment for 6 h (Figure 2B). These results indicated that **41** could disrupt the Hsp90-Cdc37 interaction in A549 cells.

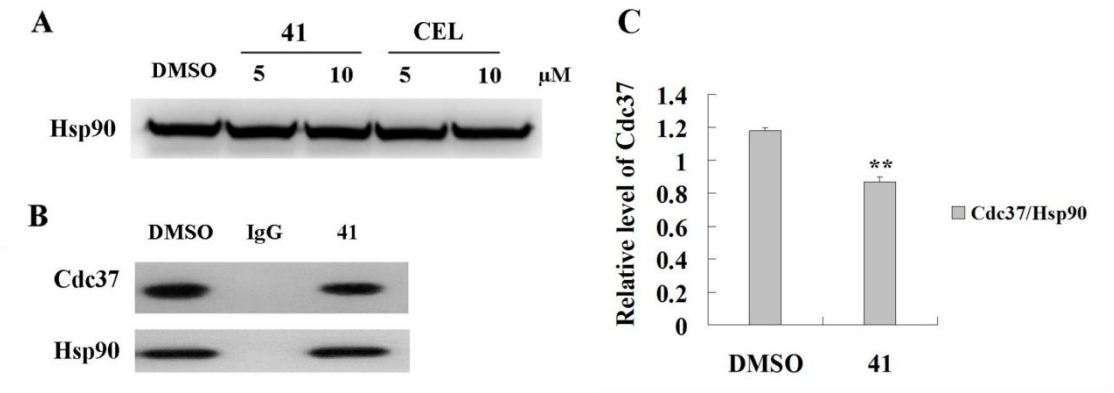

Figure 2. Effects of **41** on the level of Hsp90-Cdc37 complex *in vitro*. (A) Effects of **41** on the binding of ATP and Hsp90. Purified Hsp90α was pulled down by γ-phosphate-linked ATP-Sepharose in the presence of **41** or CEL. Hsp90α was detected by Western blot. (B) Effects of **41** on the amount of Cdc37 associated with Hsp90. A549 cells were treated with DMSO or **41** for 6 h. Cell lysate were immunoprecipitated by Hsp90α antibody. Western blot was done for detection of Hsp90 and Cdc37. (C) Quantitative analysis of co-IP. Data were expressed as the mean ± SD (n = 3). $^{**}P < 0.01$ *vs.* DMSO group.

*Comparison of the Regulations of **41** and CEL on Hsp90-Cdc37 Clients*

Furthermore, the levels of the Hsp90-Cdc37 clients induced by **41** and CEL were compared. As shown in Figure 3A, **41** and CEL both inhibited the expression of p-Akt and Cdk4 at a concentration of 5 μM. The inhibitory activity of **41** was higher than that of CEL at the same concentration (Figure 3B). These results indicated that the capability of **41** to disrupt the Hsp90-Cdc37 interaction was stronger than that of CEL.

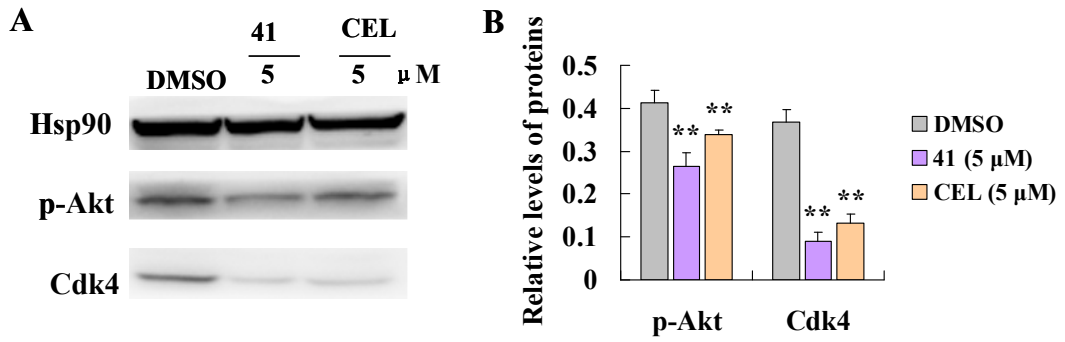

Figure 3. Effects of **41** and CEL on Hsp90-Cdc37clients. A549 cells were treated with DMSO, **41** and CEL for 12 h, and the relative levels of p-Akt and Cdk4 expression were determined by Western blot assays using Hsp90 as a control. Data are representative images and expressed as the means ± SD of each group of cells from three separate experiments. (A) Western blot analysis of the relative levels of p-AKT and Cdk4 expression. (B) Quantitative analysis. $^{**}P < 0.01$ *vs.* the DMSO group.

41 Combined with Cdc37

A previous study reported that CEL might disrupt the Hsp90-Cdc37 interaction by binding to Cdc37.[11,12] To determine whether **41** could play the same role, we first designed and synthesized an affinity probe (**41-Bio**) based on the structure of **41** to verify the binding capacity of **41** to Cdc37. The structure and synthetic route of **41-Bio** is shown in Scheme 2. As shown in Figure 4, Cdc37 was pulled down by **41-Bio**, and **41** could compete with **41-Bio** in this assay. These results indicated that **41** could bind to Cdc37 directly.

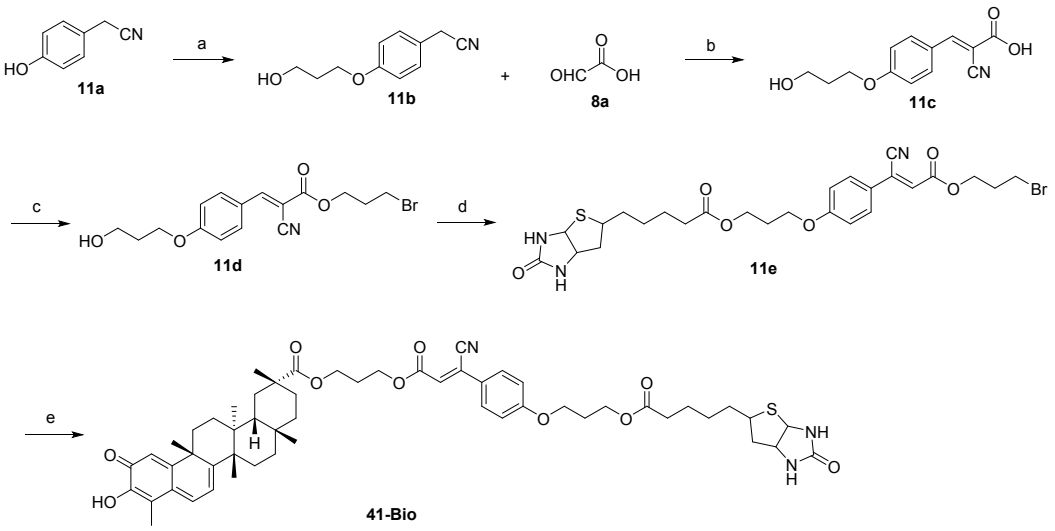

Scheme 2. Reagents and Conditions: (a) 3-bromo-1-propanol, K_2CO_3, acetone, reflux, overnight; (b) K_2CO_3, CH_3OH, 70 °C, 6 h; (c) 1,3-dibromopropane, K_2CO_3, acetone, reflux, overnight; (D) Biotin, DCC, DMAP, DMF, 30 °C, 24 h. (e) CEL, $NaHCO_3$, DMF, 60 °C, 12 h.

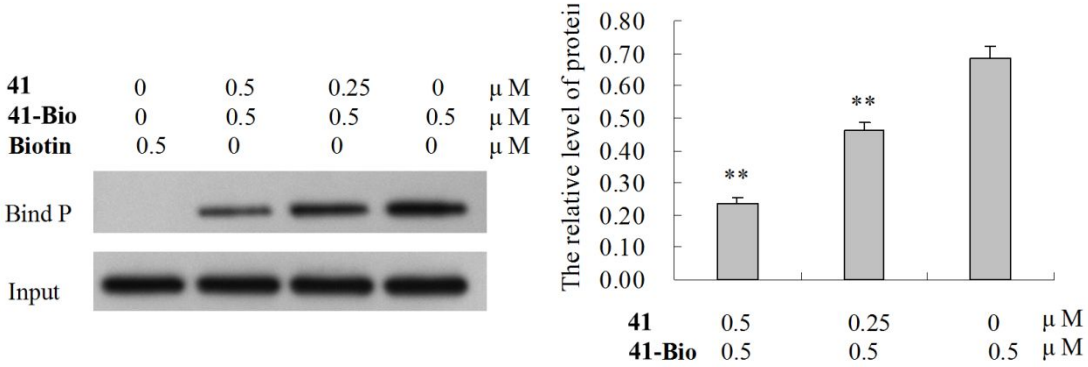

Figure 4. 41-Bio binds to Cdc37. The recombinant Cdc37 protein (5 mg) were incubated with different concentrations of **41** for 2 h before or after incubated with **41-Bio** (0.5 μM) for 2 h, and then pulled down using streptavidin beads. The total proteins (input), bound proteins (Bind P) were immunoblotted. Data were expressed as the mean ± SD (n = 3).**$P < 0.01$ *vs.* **41** (0.5 μM) group.

*Compound **41** Possessed a Higher Affinity for Cdc37 than Hsp90*

To further evaluate the protein binding ability of **41**, the combination of **41**,

Cdc37 and Hsp90 was detected by a UV method. This method was carried out by the characteristics that bound thiol groups in proteins cause the UV absorption at 440 nm to disappear, as would be the case upon binding to **41** (A, B rings). First, we needed to confirm whether the CA moiety of **41** could interfere with the reaction. The addition of **41** to dithiothreitol (DTT) was monitored by ^{1}H-NMR. As shown in Figure 5 (Fig. S151, 152), the unsaturated hydrogen signal from the CA moiety was retained (green), indicating that the CA moiety did not affect the addition of the thiol group to **41**.

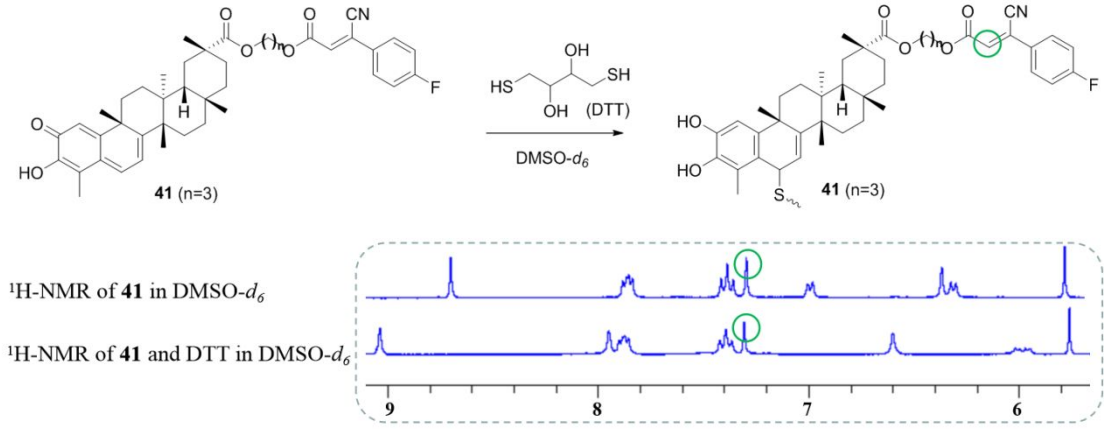

Figure 5. Overlay of ^{1}H NMR spectrum of **41** with and without DL-Dithiothreitol (DTT) in DMSO-d_6. **41** (0.02 mmol) and DTT (0.04 mmol) were dissolved in DMSO-d_6. Then ^{1}H NMR spectrum of the mixture was detected after reaction in ultrasound for 20 min.

Based on the results proposed above, **41** was added to the purified Hsp90α (full length) and Cdc37 (full length) respectively, and the UV spectrum of **41** (200-500 nm) was detected *vs*. time. Glutathione (GSH) was used as a positive control. As shown in Figure 6A, both GSH, Cdc37 and Hsp90 reduced the UV absorption of **41** at 440 nm, indicating that all of three molecules could bind to **41**. Analysis of the UV assay (Figure 6B) showed that the binding of **41** to Cdc37 reached equilibrium within 5 min,

while the combination of **41** and Hsp90 needed 15 min to equilibrate, indicating that **41** possessed a higher affinity to Cdc37 than Hsp90. These results suggested that the combination of **41** and cysteine (Cys) possessed poorly selectivity in PBS. However, under physiological conditions, **41** might reach the target protein finally as the reversibility of the reaction.[28] Therefore, **41** might disrupt the interaction of the Hsp90-Cdc37 complex by preferentially binding to Cdc37 in cancer cells.

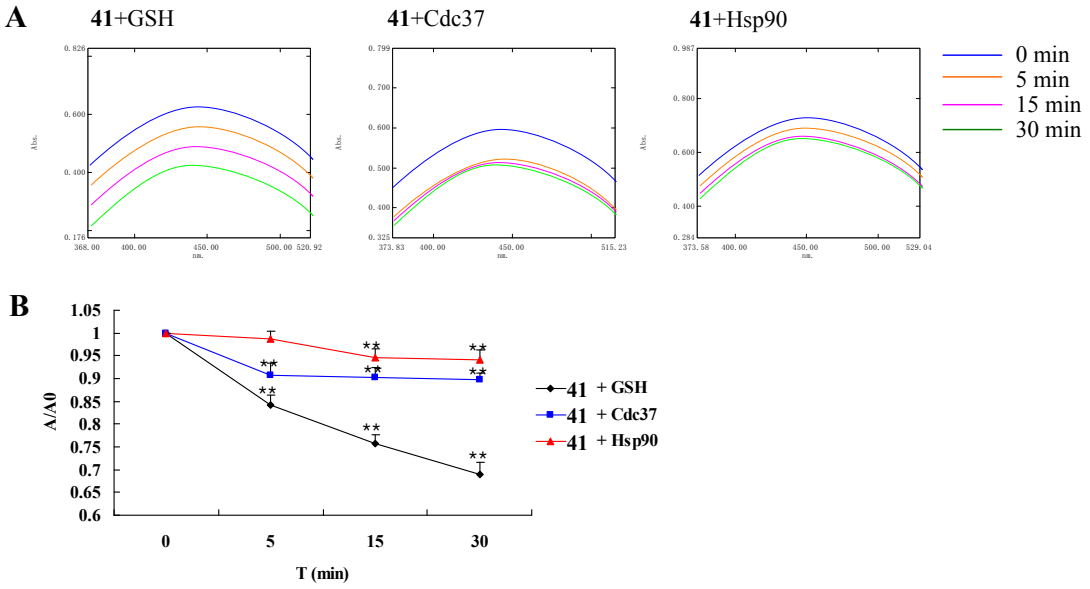

Figure 6. UV spectrum of **41** monitored after addition of GSH, Cdc37 and Hsp90. **41**(100 μM) and GSH (100 μM) or Cdc37 (1.5 μM) or Hsp90 (1.5 μM) were dissolved in PBS (1% DMSO) respectively. Then the solution was incubated at 37 °C for 0, 5, 15 and 30 min. The UV spectrum of the solution (200-500 nm) was monitored. (A) UV spectrum of **41** was monitored after incubation with GSH, Cdc37 and Hsp90. (B) Analysis of the UV assay. A0, absorbance of the solution at 440 nm with 0 min. A, absorbance of the solution at 440 nm with the corresponding time. Data were expressed as the mean ± SD (n = 3).**$P < 0.01$ *vs.* 0 min group.

*Molecular Docking of **41** to the $Hsp90_N$-$Cdc37_M$ Complex*

To further investigate the mechanism of **41** inhibiting Hsp90-Cdc37 interaction, molecular docking was first carried out to mimic the interaction between **41** (Figure 7A) and the hydrophobic pocket of the human $Hsp90_N$-$Cdc37_M$ protein complex (PDB ID: 2K5B).[12] As shown in Figure 7B, **41** was docked in the hydrophobic pocket of $Hsp90_N$-$Cdc37_M$. Four H-bonds might be formed, including between the β-CN group of the CA moiety of **41** and R166 of Cdc37 (yellow, Figure 7B), the carbonyl group of the CEL moiety and W168 of Cdc37 (purple, Figure 7B) and the carbonyl group of the CA moiety (Figure 7B) and R166 (H-bond×2). These hydrogen bonds might allow **41** efficiently disrupt the key interaction (hydrogen bonds between $Q133^{Hsp90}$ and $R166/R167^{Cdc37}$) of the $Hsp90_N$-$Cdc37_M$ by binding to Cdc37 (non-covalent bond), thereby affecting the stability of Hsp90-Cdc37.

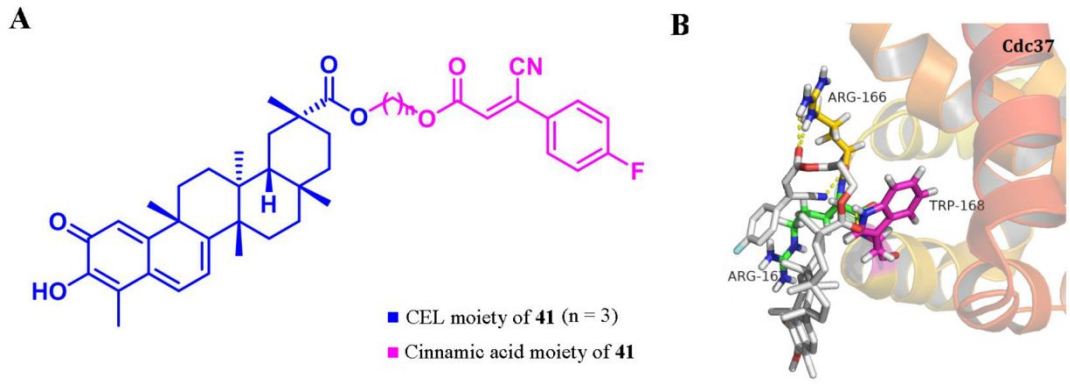

Figure 7. Molecular docking of **41** to $Hsp90_N$-$Cdc37_M$. (A) Chemical structure of **41**. (B) Binding mode of **41** with the $Hsp90_N$-$Cdc37_M$ complex (PDB ID 2K5B). The complex was shown in a cartoon representation. The side chain R166 (yellow), R167 (green) and W168 (purple) of $Cdc37_M$ and **41** (gray) were shown in a stick type. The expected hydrogen bonds were indicated by the dashed yellow lines.

***41** might form a covalent bond with C203 of $Cdc37_M$*

The reaction between quinone methide (A, B rings) and cysteine (Cys) has been considered as a key factor for the high activity of CEL derivatives. As Jiang. et al report, CEL derivatives might form a covalent bond with C203 of Cdc37 to disrupt the interaction of the Hsp90-Cdc37.[12] In order to investigate the potential mechanism of **41** inhibiting the Hsp90-Cdc37 interaction, the A,B rings were further modified (**41-H**, Figure 8, Scheme S1). As shown in Figure 8, the inhibition rate of **41-H** (20.5 %) was decreased compared to that of **41** (65.1 %) and the mixture of **41** and Methyl thioglycolate (68.3 %) in A549 at 0.5 μM. These results indicated that the A, B rings were critical for the activity of **41**. Therefore, **41** might inhibit the activity of Hsp90 by the combination between A, B rings and Cys in the Hsp90-Cdc37 complex. This complex depends on a hydrophobic interaction which is mainly located in a hydrophobic core between $Hsp90_N$ and $Cdc37_M$. And $Hsp90_N$ does not contain any Cys residues, while $Cdc37_M$ shows two Cys residues (C183 and C203) on the protein surface. As shown in Figure 9A, C183 is inaccessible as it is located in the depression on the protein surface. However, the position of C203 closes to the hydrophobic core (cyans) in Cdc37 and is more easily approached by the compounds (Figure 9B). Therefore, **41** most likely to combine with $C203^{Cdc37}$ by covalent bond to disrupt the interaction of the Hsp90-Cdc37 complex.

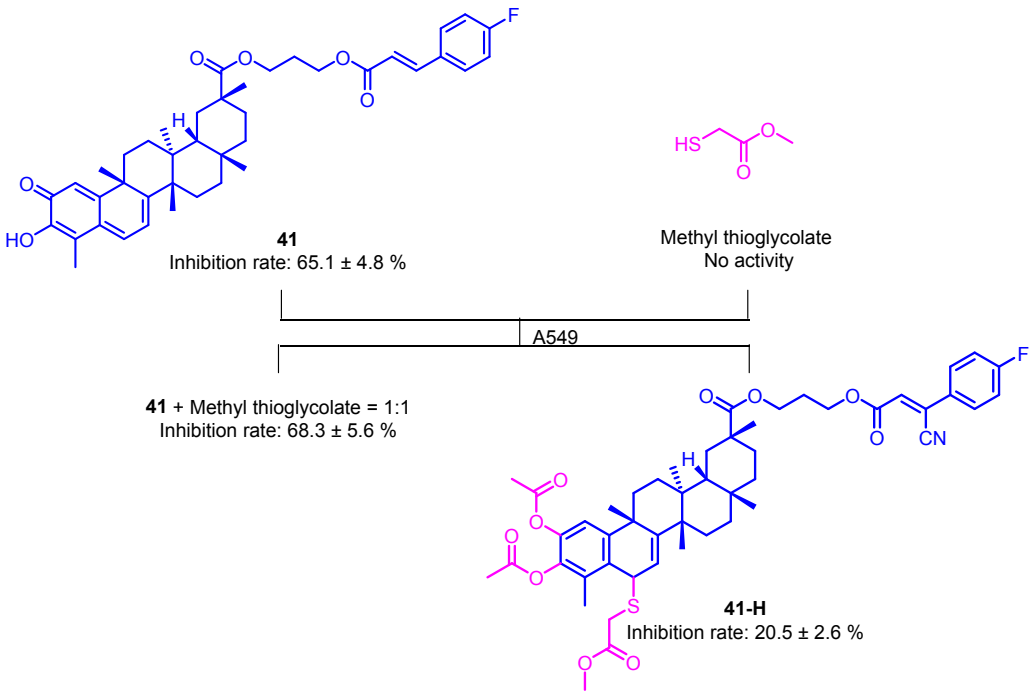

Figure 8. Anti-proliferative activity of **41-H** in comparison with that of **41**, methyl thioglycolate and the mixture of **41** and methyl thioglycolate in A549 cells.

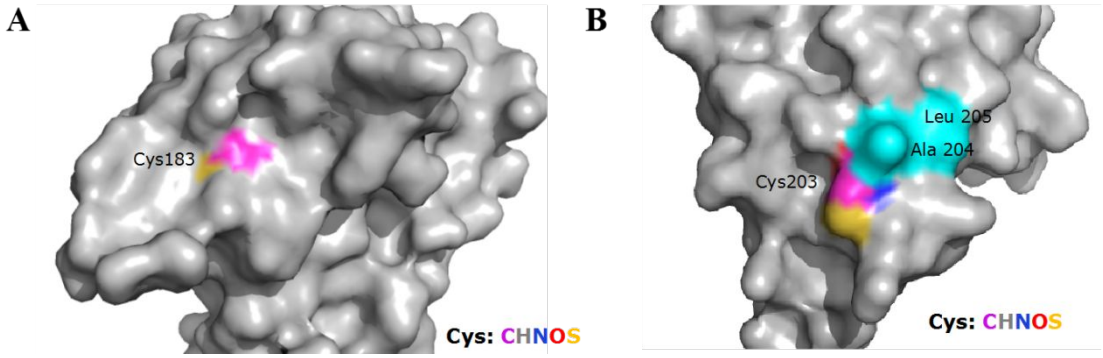

Figure 9. The structure of $Cdc37_M$ (PDB ID 2W0G). (A) The location of Cys183. (B) The location of Cys203.

*Compound **41** Regulated the Hsp90-Cdc37 Clients and Apoptosis-related Proteins*

Based on prophase research, **41** could be considered sa an Hsp90-Cdc37 disruptor. Disruption of Hsp90 and Cdc37 will down-regulates the levels of Hsp90-Cdc37 clients, resulting in the induction of apoptosis-related proteins.[29] Thus,

the effects of **41** on the levels of Hsp90-Cdc37 clients and apoptosis-related proteins were detected. As important clients of Hsp90-Cdc37, Cdk4 and p-Akt were selected to measure by Western blotting. These proteins were tested after treatment with **41** in A549 cells. As shown in Figure 10A, **41** down-regulated the levels of p-Akt and Cdk4 in a dose-dependent manner. The levels of Bax and cleaved caspase-3 were significantly increased. In contrast, as an anti-apoptotic protein, Bcl-2 expression was inhibited (Figure 10B). These results indicated that **41** regulated the levels of Hsp90-Cdc37 clients and the apoptosis-related proteins to induce cell apoptosis.

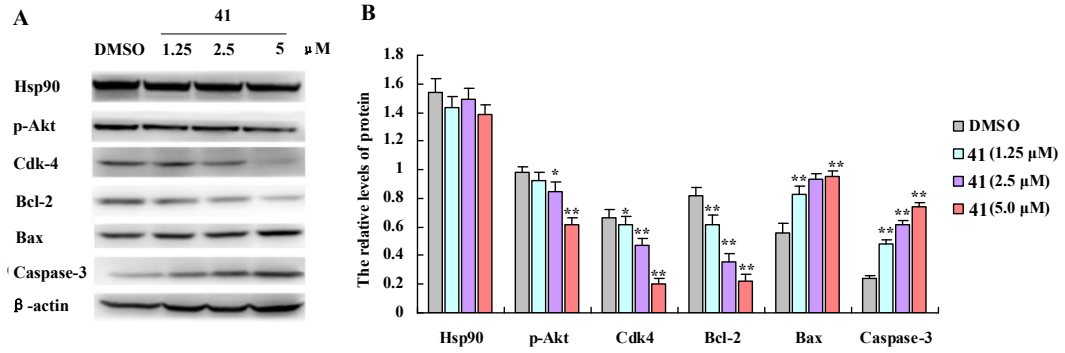

Figure 10. Effects of **41** on clients of Hsp90-Cdc37 and apoptosis-related proteins in A549 cells. A549 cells were treated with DMSO or **41** for 12 h, and the relative levels of Hsp90, p-AKT, Cdk4, Bcl-2, Bax and Caspase-3 expression were determined by Western blot assays using β-actin as a control. Data are representative images and expressed as the means ± SD of each group of cells from three separate experiments. (A) Western blot analysis of the relative levels of Hsp90, p-Akt, Cdk4, Bcl-2, Bax and Caspase-3 expression. (B) Quantitative analysis. $*P < 0.05$, $**P < 0.01$, vs the DMSO-treated control group.

*Compound **41** Decreased the Mitochondrial Membrane Potential ($\Delta\psi_m$)*

As mentioned above, **41** could regulate the levels of Hsp90 clients and apoptosis-related proteins to induce cell apoptosis. Changes in the $\Delta\psi_m$ are hallmark events of early apoptosis, regardless of whatever the apoptosisit is extrinsic apotosis or intrinsic apoptosis. Thus, to investigate the influence of **41** on the $\Delta\psi$m, JC-1 staining was used in A549 cells. As shown in Figure 11 A & B, an increase in the cell number with J-monomers (green fluorescence, depolarized mitochondria) and a concurrent decrease in the cell number with Jaggregates (red fluorescence, indicating hyperpolarized mitochondria) were exhibited in this assay. In addition, a significant loss in the $\Delta\psi$m was induced by treatment of **41** at 0.2 μM, which indicated that **41** could significantly induce apoptosis in A549 cells at a low concentration.

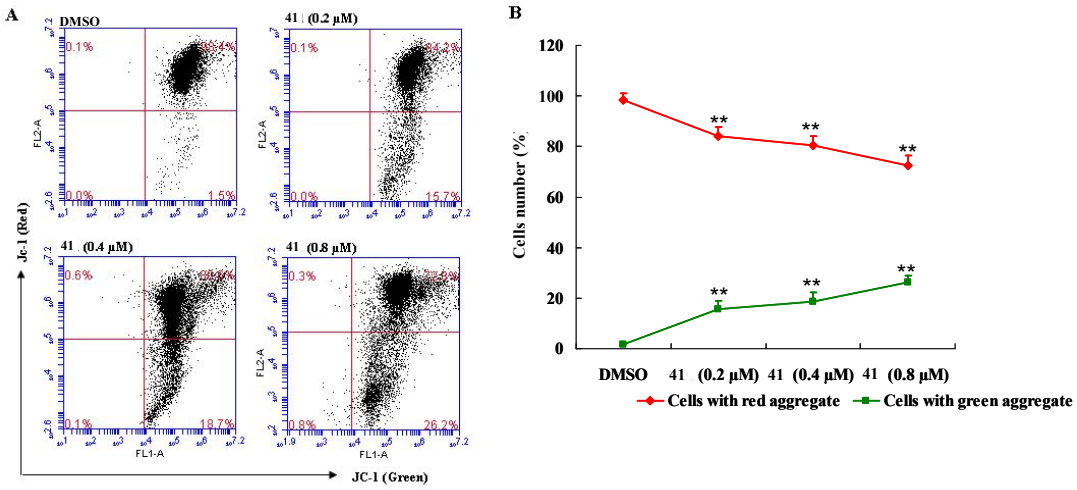

Figure 11. Effects on $\Delta\psi_m$ of **41** in A549 cells. A549 cells were treated with DMSO or **41** for 24 h and then analyzed by fluorescence microscopy and flow cytometry after JC-1 staining. (A) Flow cytometry analysis of A549 cells treated with DMSO and **41**. (B) The quantification of cells (%) with red and green aggregates. The values are presented as mean ± SD (n = 3). $^{**}P < 0.01$ *vs.* the DMSO group.

*The Morphological Apoptosis Induced by **41***

Next, the morphological apoptosis induced by **41** was detected by Hoechst 33342 and propidium iodide (PI) staining. Hoechst 33342 stained the apoptotic cells bright blue, and PI stained the dead cells red. As shown in Figure 12, the cell density decreased significantly as drug concentration increased. Simultaneously, the number of apoptotic cells were increased. The characteristics of apoptotic cells were observed in apoptotic cells (white arrows), such as nuclear fragmentation and chromatin condensation.

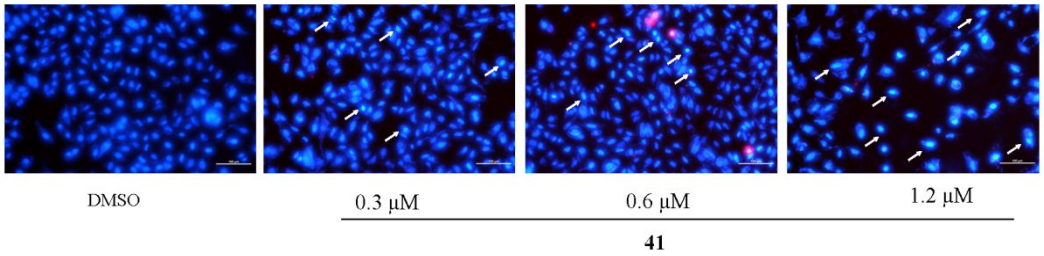

Figure 12. The morphological apoptosis induced by **41** in A549. A549 cells were treated with **41** or DMSO for 48 h. Fluorescence microscopy images of A549 cells stained by Hoechst 33342 and PI. The apoptotic cells were stained by Hoechst 33342 in bright blue and the dead cells were stained by PI in red.

*Effects of **41** on Cell Apoptosis*

To examine whether apoptosis was induced by **41** , an annexin V-FITC/PI dual staining assay was performed in A549 cells. As shown in Figure 13A, after 48 h of treatment with **41**, significant apoptosis was induced in a dose-manner, especially in late apoptotic cells (9.3%, 16.9% and 25.2% at the concentrations). Furthermore, at a concentration of 1.2 μM, the apoptotic cells induced by treatment with **41** accounted for 32.6% of the cells, which was higher than that of CEL (23.1%) (Figure 13B). These results suggested that the superior activity of **41** might be mainly through an

apoptotic pathway.

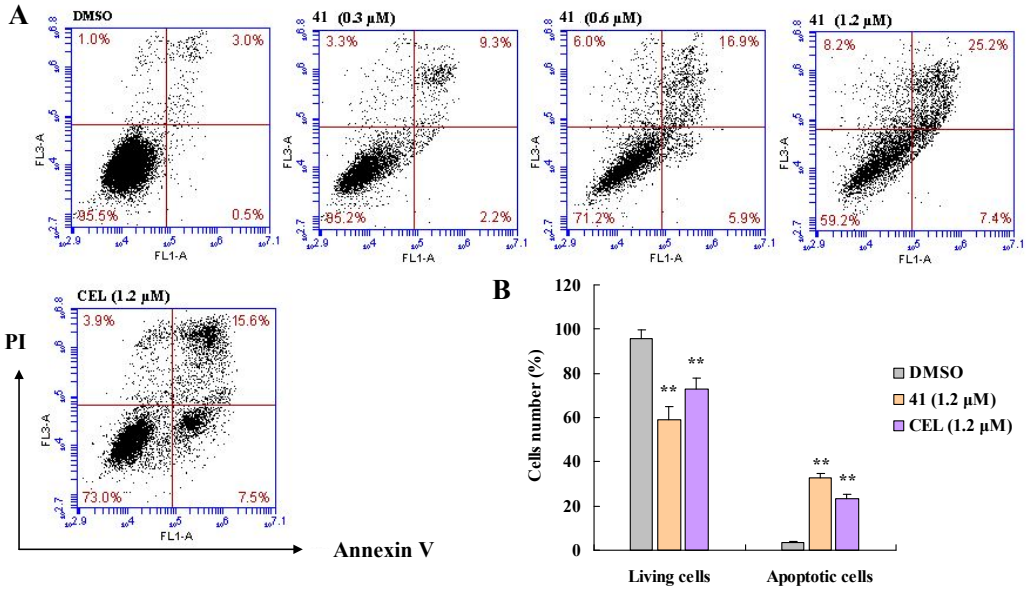

Figure 13. Apoptotic effects of **41** and CEL in A549 cells. Treatment with DMSO or **41** or CEL for 48 h, A549 cells were collected and stained with Annexin V/PI, followed by flow cytometric analysis. (A) Flow cytometry analysis of A549 cells treated with DMSO, **41** and CEL. (B) Representative histograms for the numbers of living cells and apoptotic cells (%). The values were presented as the mean ± SD (n = 3). $^{**}P < 0.05$ *vs.* the DMSO group.

*Effects of **41** on the Cell Cycle*

Cdk4 is a key regulator of the cell cycle. Inhibition of Cdk4 expression will arrest the cell cycle in the G_0/G_1 phase. Western blotting verified that **41** could decrease the amount of Cdk4. Thus, we further investigated the effects of **41** on cell cycle progression. As shown in Figure 14A & B, **41** arrested the cell cycle in the G_0/G_1 phase in a dose-dependent manner in A549 cells. These results indicated that the effects of **41** on the cell cycle were another pathway that induced the apoptosis in cancer cells.

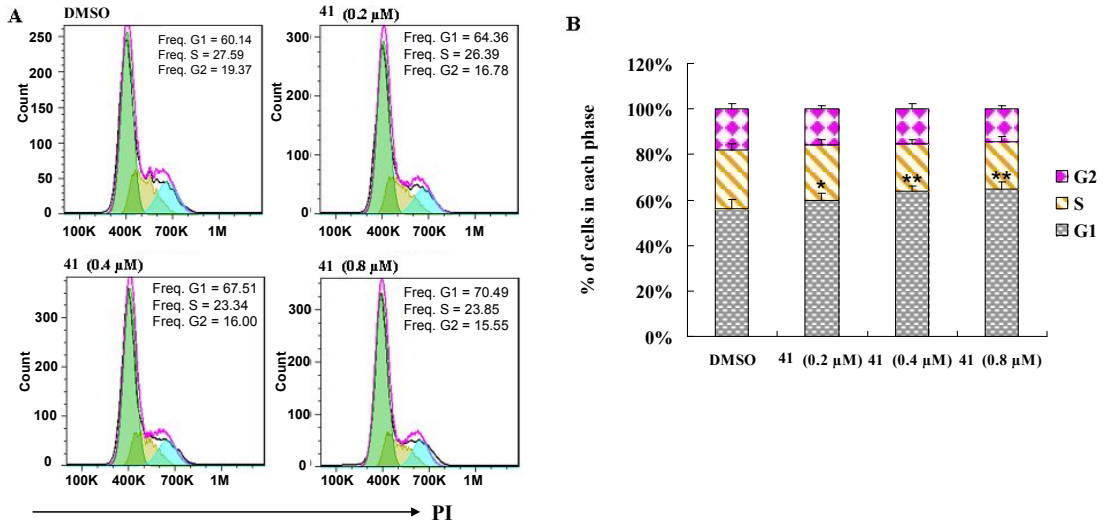

Figure 14. Effect of **41** on cell cycle progression of A549 cells. Treatment of A549 cells with DMSO and **41** (0.2, 0.4 and 0.8 μM) for 24 h, intracellular DNA was stained with PI. Cell cycle distribution was analyzed by flow cytometry. (A) Flow cytometry analysis of cell cycle distribution of **41** on A549. (B) The quantification of cells (%) in each cell phase. The values are presented as mean ± SD (n = 3). *$P < 0.01$, **$P < 0.05$ *vs.* the DMSO group.

Conclusion

Based on the analysis of the $Hsp90_N$-$Cdc37_M$ structure, lipophilic fragments with small molecules (CA and α- or β-CN substituted CA) were introduced into CEL to synthesize 48 new derivatives. Their anti-proliferative activities were evaluated against four cancer cell lines (A549, HOS, MCF-7 and HepG2) and the SAR of these derivatives was discussed. Further study showed that **41** disrupted the interaction of the Hsp90-Cdc37 complex in A549 cells. Molecular docking analysis indicated that **41** might inhibit the interaction of Hsp90-Cdc37 by binding to Cdc37, and **41** bound to Cdc37 more efficiently than Hsp90 in UV assay. Pharmacological studies showed

that **41** could regulate the levels of Hsp90-Cdc37 clients and the apoptosis-related proteins to induce the cell cycle arrest and the apoptosis in A549 cells. Jiang's study indicated that introduction of the polar groups in C29-carboxyl of CEL were favorable on Hsp90-Cdc37 disruption. However, a suitable hydrophobic group could also enhance Hsp90-Cdc37 disruption activity when introduced to this site in our and previous study. These results suggested that mechanism of disrupting the Hsp90-Cdc37 interaction by small molecules was complex. The binding capability is not only related to the polar of the compound's structure, but also the spatial structure, flexibility and electrical properties, etc. Overall, **41** displayed superior anti-proliferative activity against cancer cells by disrupting the interaction of Hsp90-Cdc37 by preferentially binding to Cdc37 (hydrogen bond and/or covalent bond). The current finding may provide new insight into the design of CEL derivatives as novel Hsp90-Cdc37 disruptors.

EXPERIMENTAL PROTOCOLS

(1) Chemical Analysis. Celastrol was purchased from Tuochukangyuan company (Hubei, China). Synthetic reagents were purchased from chemical and biological company. The following antibodies used for immunoprecipitation and western blotting (Hsp90α, Cdc37; Hsp90, p-Akt, Cdk4, Bcl-2, Bax and Caspase 3) were purchased from Abcam. The purity of all tested compounds was characterized by HPLC analysis (LC-2030C HPLC system consisting of LC-2030C pumps and an SPD-2030C UV detector). Individual compounds with a purity of >95% were used for subsequent experiments (see Supporting Information).

(2) General Procedures for the Preparation of Compounds 2f-t. 1a/1b/1c/1d/1e (1.2 mmol, 1.2 eq), EDCI (288.0 mg, 1.5 mmol, 1.5 eq) and DMAP (61.0 mg, 1.0 mmol, 0.5 eq) were successively added to a solution of bromohydrin (1.0 mmol, 1.0 eq) in CH_2Cl_2 (6 ml) and this reaction mixture was stirred for 7 h at room temperature. The reaction mixture was concentrated under vacuum and the residue was dissolved in CH_2Cl_2. The organic layer was washed with 5% aqueous $NaHCO_3$ solution (60 ml) and aqueous saturated NaCl solution (30 ml). After drying over anhydrous Na_2SO_4, the CH_2Cl_2 was removed in vacuum. The crude materials was purified by column chromatography on silica gel [petroleum ether (PE)/ethyl acetate (EA) = 16:1 (v/v)] to afford pure compounds **2f-t**.

(3) General Procedures for the Preparation of Compounds 5a-e. NH_4OAc (577.5 mg, 7.5 mmol, 0.5 eq) and different aryl aldehydes **3a-e** (13.5 mmol, 0.9 eq) were dissolved in a solution of **4a** (15.0 mmol, 1 eq, 1.28g) in tolune (45 ml). The mixture was heated at 100℃ for 12 h. The reaction mixture was filtered to afford the crude product **5a-5e**.

(4) General Procedures for the Preparation of Compounds 6f-t. 6f-6t were synthesized from **5a-5e** by using the methods employed in the case of **2f-2t**. The crude materials was purified by column chromatography on silica gel [PE/EA=16:1 (v/v)] to achieve **6f-t**.

(5) General Procedures for the Preparation of Compounds 9a-e. K_2CO_3 (3.11 g, 22.5 mmol, 1.5 eq) and different aryl acetonitriles **7a-e** (15.0 mmol, 1.0 eq) were added to a solution of **8a** (1.11 g, 15.0 mmol, 1.0 eq) in CH_3OH (50 ml). The mixture

was refluxed at 60 °C for 6 h. The reaction mixture was filtered and the filter cake was washed by CH_2Cl_2 and then dissolved in water. The solution was acidified using 1 M hydrochloric acid solution to pH = 4 and filtered. The filter cake was the crude product **9a-e**.

(6) General procedures for synthesizing compounds 10f-t. **10f-10t** were synthesized from **9a-e** by using the methods employed in the case of **2f-2t**. The crude materials were separated by column chromatography on silica gel [PE/EA=16:1 (v/v)] to achieve **10f-t**.

(7) General procedures for synthesizing compounds 10u-w. **9a/9c/9d** (0.5 mmol, 1.0 eq), K_2CO_3 (138.0 mg, 1.0 mmol, 2.0 eq), $Bu_4N^+Br^-$ (9.7 mg, 0.06 eq, 0.03 mmol) and trans-1,4-dibromo-2-butene (321.0 mg, 1.5 mmol, 3.0 eq) were added into anhydrous acetone. The reaction mixture was refluxed for 7 h at 60 °C. The acetone was removed under reduced pressure and the residue was extracted with ethyl acetate (60 ml). The combined organic layers were dried over sodium sulfate, filtered, and the solvent was evaporated. The crude materials were purified by column chromatography on silica gel [PE/EA = 16:1 (v/v)] to afford **10u-w**.

(8) General Procedures for the Preparation of Target Compounds 1-48. A mixture of CEL (45.1 mg, 0.1 mmol, 1.0 eq), **2a-o** or **6a-o** or **10a-r** (0.3 mmol, 3.0 eq) and $NaHCO_3$ (42.0 mg, 0.5 mmol, 5.0 eq) in anhydrous DMF (6 ml) was stirred at 60 °C for 7 h. The reaction solution was washed with CH_2Cl_2 (100 ml) for four times. The combined organic layers were washed by aqueous saturated NaCl solution (30 ml), and then dried over sodium sulfate, filtered, and the solvent was evaporated. The

crude product was purified by column chromatography [PE/EA = 6:1 (v/v)].

Compound **1**. Orange powder, 55% yield. M.p. 149.3-151.7 °C; ^{1}H NMR (300 MHz, $CDCl_3$) δ_H: 0.58 (3H, s), 1.11 (3H, s), 1.22 (3H, s), 1.26 (3H, s), 1.43 (3H, s), 2.21 (3H, s), 4.08-4.12 (1H, m), 4.30-4.46 (3H, m), 6.26 (1H, d, *J* = 7.1 Hz), 6.44 (1H, d, *J* = 16.0 Hz), 6.52 (1H, s), 6.95 (1H, d, *J* = 7.1 Hz), 7.43 (3H, m), 7.55 (2H, m), 7.72 (1H, d, *J* = 16.1 Hz); ^{13}C NMR (75 MHz, $CDCl_3$) δ_C: 178.2 (C×2), 169.9, 166.8, 164.6, 146.0, 145.1, 134.2, 134.1, 130.3, 128.9 (C×2), 128.1 (C×2), 127.4, 119.6, 118.1, 117.7, 117.2, 61.0 (C×2), 45.1, 44.3, 42.9, 40.5, 39.4, 38.2, 36.3, 34.8, 33.4, 32.8, 31.6, 30.9, 30.5, 29.8, 29.7, 28.6, 27.7, 21.6, 18.5, 10.3. HRMS (ESI) calculated for $C_{40}H_{49}O_6$ $[M + H]^+$ 625.3529, found 625.3529.

Compound **2**. Orange powder, 51% yield. M.p. 135.2-137.1 °C; ^{1}H NMR (300 MHz, $CDCl_3$) δ_H: 0.59 (3H, s), 1.12 (3H, s), 1.22 (3H, s), 1.28 (3H, s), 1.46 (3H, s), 2.19 (3H, s), 4.01-4.15 (2H, m), 4.23-4.34 (2H, m), 6.35 (1H, d, *J* = 7.1 Hz), 6.41 (1H, d, *J* = 15.9 Hz), 6.55 (1H, s), 6.99 (1H, d, *J* = 7.1 Hz), 7.41 (3H, m), 7.49 (2H, m), 7.67 (1H, d, *J* = 15.9 Hz); ^{13}C NMR (75 MHz, $CDCl_3$) δ_C: 178.3, 178.2, 169.9, 166.5, 164.6, 146.0, 145.4, 135.0, 134.3, 130.5, 128.9 (C×2), 128.2 (C×2), 127.4, 119.3, 118.3, 117.5, 117.2, 62.3, 61.7, 45.1, 44.3, 42.9, 40.5, 39.6, 38.2, 36.3, 34.8, 33.5, 32.8, 31.6, 30.9, 30.5, 29.7, 29.6, 28.6, 21.6, 18.6, 10.3. HRMS (ESI) calculated for $C_{41}H_{51}O_6$ $[M + H]^+$ 639.3686, found 639.3686.

Compound **3**. Orange powder, 46% yield. M.p. 145.5-147.1 °C; 0.57 (3H, s), 1.10 (3H, s), 1.20 (3H, s), 1.30 (3H, s), 1.43 (3H, s), 2.21 (3H, s), 3.89-3.93 (1H, m), 4.04-4.07 (1H, m), 4.23-4.27 (2H, m), 6.34 (1H, d, *J* = 7.2 Hz), 6.46 (1H, d, *J* = 16.0 Hz), 6.54

(1H, s), 7.01 (1H, d, J = 7.2 Hz), 7.39 (3H, m), 7.55 (2H, m), 7.70 (1H, d, J = 16.0 Hz); ^{13}C NMR (75 MHz, $CDCl_3$) δ_C: 178.3 ,178.2 169.9, 166.9, 164.7, 146.0, 144.9, 134.4, 134.0, 130.0, 128.9 (C×2), 128.1 (C×2), 127.4, 119.6, 118.1, 118.0, 117.1, 64.0 (C×2), 45.0, 44.3, 42.9, 40.4, 39.4, 38.2, 36.4, 34.8, 33.5, 32.8, 31.6, 30.8, 30.6, 29.8, 29.7, 28.6, 25.6, 25.2, 21.6, 18.5, 10.3. HRMS (ESI) calculated for $C_{42}H_{53}O_6$ $[M + H]^+$ 653.2842, found 653.3842.

Compound **4**. Orange powder, 53% yield. M.p. 143.9-146.1 °C; ^{1}H NMR (300 MHz, $CDCl_3$) δ_H: 0.58 (3H, s), 1.11 (3H, s), 1.22 (3H, s), 1.26 (3H, s), 1.44 (3H, s), 2.22 (3H, s), 2.41 (3H, s), 4.08-4.13 (3H, m), 4.27-4.40 (1H, m), 6.27 (1H, d, J = 7.0 Hz), 6.39 (1H, d, J = 16.1 Hz), 6.53 (1H, s), 6.95 (1H, d, J = 7.1 Hz), 7.24 (2H, d, J = 7.9 Hz), 7.46 (2H, d, J = 7.7 Hz), 7.69 (1H, d, J = 16.0 Hz); ^{13}C NMR (75 MHz, $CDCl_3$) δ_C: 178.2 (C×2), 170.3, 166.6, 164.7, 146.0, 145.4, 141.0, 134.3, 131.6, 129.7 (C×2), 128.2 (C×2), 127.4, 119.5, 118.2, 117.2, 116.4, 62.4, 61.7, 45.1, 44.3, 43.0, 40.5, 39.5, 38.2, 36.4, 34.8, 33.5, 32.8, 31.6, 30.9, 30.5, 29.7, 29.6, 28.6, 21.6, 21.5, 18.6, 10.3. HRMS (ESI) calculated for $C_{41}H_{51}O_6$ $[M + H]^+$ 639.3686, found 639.3673.

Compound **5**. Orange powder, 47% yield. M.p. 145.8-147.6 °C; ^{1}H NMR (300 MHz, $CDCl_3$) δ_H: 0.59 (3H, s), 1.12 (3H, s), 1.21 (3H, s), 1.28 (3H, s), 1.45 (3H, s), 2.18 (3H, s), 2.39 (3H, s), 4.01-4.14 (2H, m), 4.19-4.33 (2H, m), 6.34 (1H, d, J = 7.1 Hz), 6.36 (1H, d, J = 16.0 Hz), 6.54 (1H, s), 6.97 (1H, d, J = 7.0 Hz), 7.19 (2H, d, J = 7.8 Hz), 7.39 (2H, d, J = 7.7 Hz), 7.64 (1H, d, J = 15.9 Hz); ^{13}C NMR (75 MHz, $CDCl_3$) δ_C: 178.2 ,178.1, 170.0, 167.0, 164.7, 146.0, 145.1, 140.8, 134.2, 131.5, 129.6 (C×2), 128.1 (C×2), 127.4, 119.5, 118.2, 117.2, 116.6, 61.0, 60.9, 45.1, 44.3, 43.0, 40.5, 39.5,

38.2, 36.4, 34.8, 33.4, 32.8, 31.6, 30.8, 30.5, 29.8, 29.7, 28.6, 27.9, 21.6, 21.5, 18.6, 10.3. HRMS (ESI) calculated for $C_{42}H_{53}O_6$ $[M + H]^+$ 653.3842, found 653.3845.

Compound **6**. Orange powder, 45% yield. M.p. 137.8-139.2 °C; ^{1}H NMR (300 MHz, $CDCl_3$) δ_H: 0.56 (3H, s), 1.10 (3H, s), 1.20 (3H, s), 1.26 (3H, s), 1.43 (3H, s), 2.20 (3H, s), 2.37 (3H, s), 3.87-3.95 (1H, m), 4.01-4.09 (1H, m), 4.22-4.26 (2H, m), 6.38 (1H, d, J = 7.1 Hz), 6.40 (1H, d, J = 16.0 Hz), 6.53 (1H, s), 7.00 (1H, d, J = 6.9 Hz), 7.19 (2H, d, J = 7.9 Hz), 7.43 (2H, d, J = 7.9 Hz), 7.67 (1H, d, J = 16.0 Hz); ^{13}C NMR (75 MHz, $CDCl_3$) δ_C: 178.3 ,178.2, 169.8, 167.1, 164.6, 146.0, 144.8, 140.7, 134.0, 131.7, 129.6 (C×2), 128.1 (C×2), 127.4, 119.6, 118.1, 117.1, 116.9, 64.0, 63.9, 45.0, 44.3, 42.9, 40.4, 39.4, 38.2, 36.6, 34.8, 33.5, 32.8, 31.6, 30.8, 30.5, 29.8, 29.6, 28.6, 25.6, 25.2, 21.6, 21.5, 18.5, 10.2. HRMS (ESI) calculated for $C_{43}H_{55}O_6$ $[M + H]^+$ 667.3999, found 667.3998.

Compound **7**. Orange powder, 52% yield. M.p. 144.2-146.3 °C; ^{1}H NMR (300 MHz, $CDCl_3$) δ_H: 0.58 (3H, s), 1.12 (3H, s), 1.22 (3H, s), 1.36 (3H, s), 1.44 (3H, s), 2.23 (3H, s), 3.88 (3H, s), 4.07-4.14 (1H, m), 4.28-4.43 (3H, m), 6.30 (1H, d, J = 6.5 Hz), 6.32 (1H, d, J = 15.7 Hz), 6.56 (1H, s), 7.00 (2H, d, J = 8.5 Hz), 7.01 (1H, d, J = 6.4 Hz), 7.51 (2H, d, J = 8.4 Hz), 7.67 (1H, d, J = 15.7 Hz); ^{13}C NMR (75 MHz, $CDCl_3$) δ_C: 178.3 (C×2), 169.7, 167.2, 164.7, 161.3, 146.0, 144.7, 133.9, 129.8 (C×2), 127.4, 127.1, 119.6, 118.1, 117.1, 115.3, 114.3 (C×2), 61.8, 61.0, 55.7, 45.0, 44.3, 42.9, 40.5, 39.4, 38.2, 36.4, 34.9, 33.4, 32.8, 31.6, 30.8, 30.5, 29.8 (C×2), 28.6, 21.7, 18.6, 10.2. HRMS (ESI) calculated for $C_{41}H_{51}O_7$ $[M + H]^+$ 655.3635, found 655.3618.

Compound **8**. Orange powder, 41% yield. M.p. 129.4-131.7 °C; ^{1}H NMR (300 MHz,

$CDCl_3$) δ_H: 0.59 (3H, s), 1.12 (3H, s), 1.22 (3H, s), 1.28 (3H, s), 1.46 (3H, s), 2.19 (3H, s), 3.87 (3H, s), 4.01-4.15 (2H, m), 4.27-4.40 (2H, m), 6.27 (1H, d, J = 15.9 Hz), 6.34 (1H, d, J = 6.9 Hz), 6.54 (1H, s), 6.91 (2H, d, J = 8.3 Hz), 6.98 (1H, d, J = 7.1 Hz), 7.44 (2H, d, J = 8.3 Hz), 7.61 (1H, d, J = 16.0 Hz); ^{13}C NMR (75 MHz, $CDCl_3$) δ_C: 178.3 ,178.2, 169.7, 167.1, 164.6, 161.5, 146.0, 144.7, 133.9, 129.7 (C×2), 127.4, 127.0, 119.6, 118.1, 117.0, 115.2, 114.3 (C×2), 61.0, 60.8, 55.4, 45.0, 44.3, 42.9, 40.5, 39.4, 38.2, 36.4, 34.9, 33.4, 32.8, 31.6, 30.8, 30.5, 29.8, 29.7, 28.6, 27.9, 21.7, 18.5, 10.2. HRMS (ESI) calculated for $C_{42}H_{53}O_7$ $[M + H]^+$ 669.3791, found 669.3794.

Compound **9**. Orange powder, 49% yield. M.p. 124.1-126.6 ℃; ^{1}H NMR (300 MHz, $CDCl_3$) δ_H: 0.56 (3H, s), 1.10 (3H, s), 1.20 (3H, s), 1.26 (3H, s), 1.43 (3H, s), 2.20 (3H, s), 3.84 (3H, s), 3.89-3.95 (1H, m), 4.01-4.09 (1H, m), 4.21-4.25 (2H, m), 6.32 (1H, d, J = 16.2 Hz), 6.34 (1H, d, J = 6.9 Hz), 6.53 (1H, s), 6.90 (2H, d, J = 8.7 Hz), 7.00 (1H, d, J = 7.1 Hz), 7.49 (2H, d, J = 8.7 Hz), 7.65 (1H, d, J = 15.9 Hz); ^{13}C NMR (75 MHz, $CDCl_3$) δ_C: 178.3 ,178.2, 169.9, 167.2, 164.7, 161.4, 146.0, 144.5, 134.0, 129.8 (C×2), 127.4, 127.1, 119.6, 118.1, 117.1, 115.5, 114.3 (C×2), 64.0, 63.9, 55.4, 45.0, 44.2, 42.9, 40.4, 39.4, 38.2, 36.4, 34.8, 33.5, 32.8, 31.6, 30.8, 30.5, 29.8, 29.6, 28.6, 25.7, 25.2, 21.6, 18.5, 10.2. HRMS (ESI) calculated for $C_{43}H_{55}O_7$ $[M + H]^+$ 683.3948, found 683.3952.

Compound **10**. Orange powder, 54% yield. M.p. 138.0-140.7 ℃; ^{1}H NMR (300 MHz, $CDCl_3$) δ_H: ^{1}H-NMR (300 MHz, $CDCl_3$, TMS), δ ppm: 0.58 (3H, s), 1.11 (3H, s), 1.21 (3H, s), 1.26 (3H, s), 1.44 (3H, s), 2.21 (3H, s), 4.09-4.11 (1H, m), 4.28-4.44 (3H, m), 6.27 (1H, d, J = 15.9 Hz), 6.35 (1H, d, J = 7.2 Hz), 6.51 (1H, s), 6.98 (1H, d, J =

7.2 Hz), 7.12 (2H, t, *J* = 8.6 Hz), 7.54 (2H, t, *J* = 8.6 Hz), 7.76 (1H, d, *J* = 16.1 Hz); ^{13}C NMR (75 MHz, $CDCl_3$) δ_C: 178.1 (C×2), 170.1, 166.3, 164.7, 162.3, 146.1, 144.1, 134.1, 130.1, 130.0 (C×2), 127.4, 119.5, 118.1, 117.7, 117.3, 116.3, 116.0, 62.3, 61.9, 45.0, 44.2, 43.0, 40.5, 39.4, 38.2, 36.3, 34.8, 33.5, 32.8, 31.6, 30.8, 30.5, 29.7, 29.6, 28.6, 21.6, 18.6, 10.3. HRMS (ESI) calculated for $C_{40}H_{48}FO_6$ $[M + H]^+$ 643.3435, found 643.3434.

Compound **11**. Orange powder, 44% yield. M.p. 133.9-142.1 °C; ^{1}H NMR (300 MHz, $CDCl_3$) δ_H: 0.57 (3H, s), 1.11 (3H, s), 1.20 (3H, s), 1.29 (3H, s), 1.43 (3H, s), 2.17 (3H, s), 3.99-4.13 (2H, m), 4.21-4.26 (1H, m), 4.31-4.36 (1H, m), 6.30 (1H, d, *J* = 15.9 Hz), 6.34 (1H, d, *J* = 6.0 Hz), 6.54 (1H, s), 6.98 (1H, d, *J* = 6.1 Hz), 7.06 (2H, t, *J* = 8.5 Hz), 7.46 (2H, m), 7.60 (1H, d, *J* = 16.1 Hz); ^{13}C NMR (75 MHz, $CDCl_3$) δ_C: 178.2 (C×2), 170.0, 166.6, 164.7, 162.2, 146.0, 143.7, 134.1, 130.0, 129.9 (C×2), 127.4, 119.5, 118.2, 117.5, 117.2, 116.2, 115.9, 61.0 (C×2), 45.1, 44.3, 43.0, 40.5, 39.4, 38.2, 36.3, 34.8, 33.4, 32.8, 31.6, 30.8, 30.5, 29.8, 29.7, 28.6, 27.9, 21.7, 18.5, 10 . HRMS (ESI) calculated for $C_{41}H_{50}FO_6$ $[M + H]^+$ 657.3591, found 657.3593.

Compound **12**. Orange powder, 52% yield. M.p. 142-144.9 °C; ^{1}H NMR (300 MHz, $CDCl_3$) δ_H: 0.57 (3H, s), 1.11 (3H, s), 1.20 (3H, s), 1.27 (3H, s), 1.44 (3H, s), 2.21 (3H, s), 3.90-3.95 (1H, m), 4.04-4.10 (1H, m), 4.23-4.26 (2H, m), 6.35 (1H, d, *J* = 7.0 Hz), 6.47 (1H, d, *J* = 15.9 Hz), 6.54 (1H, s), 7.01 (1H, d, *J* = 7.0 Hz), 7.09 (2H, t, *J* = 8.6 Hz), 7.54 (2H, m), 7.67 (1H, d, *J* = 16.1 Hz); ^{13}C NMR (75 MHz, $CDCl_3$) δ_C: 178.4, 178.2, 170.0, 166.5, 164.7, 162.2, 146.0, 143.6, 134.0, 130.0, 129.9 (C×2), 127.4, 119.5, 118.2, 117.8, 117.2, 116.2, 115.9, 64.1, 64.0, 45.0, 44.2, 42.9, 40.4, 39.4,

38.2, 36.3, 34.8, 33.5, 32.8, 31.6, 30.8, 30.6, 29.8, 29.7, 28.6, 25.6, 25.2, 21.6, 18.5, 10.2. HRMS (ESI) calculated for $C_{42}H_{52}FO_6$ $[M + H]^+$ 671.3748, found 671.3746.

Compound **13**. Orange powder, 43% yield. M.p. 144.5-145.9 °C; ^{1}H NMR (300 MHz, $CDCl_3$) δ_H: 0.58 (3H, s), 1.12 (3H, s), 1.22 (3H, s), 1.27 (3H, s), 1.44 (3H, s), 2.21 (3H, s), 4.13-4.17 (1H, m), 4.29-4.40 (3H, m), 6.29 (1H, d, J = 7.1 Hz), 6.51 (1H, s), 6.53 (1H, d, J = 15.9 Hz), 6.97 (1H, d, J = 7.1 Hz), 7.66 (4H, m), 7.73 (1H, d, J = 16.0 Hz); ^{13}C NMR (75 MHz, $CDCl_3$) δ_C: 178.0 (C×2), 169.9, 166.0, 164.8, 146.0, 143.5, 137.6, 134.5, 128.3 (C×3), 127.4, 125.9 (C×2), 124.2, 120.1, 119.4, 118.2, 117.2, 62.1 (C×2), 45.0, 44.2, 43.1, 40.5, 39.5, 38.3, 36.3, 34.8, 33.5, 32.7, 31.6, 30.8, 30.6, 29.7, 29.6, 28.6, 21.6, 18.7, 10.2. HRMS (ESI) calculated for $C_{41}H_{48}F_3O_6$ $[M + H]^+$ 693.3403, found 693.3408.

Compound **14**. Orange powder, 55% yield. M.p. 147.3-149.0 °C; ^{1}H NMR (300 MHz, $CDCl_3$) δ_H: 0.59 (3H, s), 1.12 (3H, s), 1.22 (3H, s), 1.28 (3H, s), 1.46 (3H, s), 2.17 (3H, s), 4.03-4.11 (2H, m), 4.24-4.29 (1H, m), 4.35-4.40 (1H, m), 6.35 (1H, d, J = 7.1 Hz), 6.47 (1H, d, J = 16.1 Hz), 6.54 (1H, s), 6.99 (1H, d, J = 7.2 Hz), 7.58 (2H, d, J = 8.6 Hz), 7.65 (2H, d, J = 8.8 Hz), 7.66 (1H, d, J = 16.0 Hz); ^{13}C NMR (75 MHz, $CDCl_3$) δ_C: 178.2 (C×2), 170.1, 166.1, 164.7, 146.0, 143.1, 137.8, 134.1, 128.2 (C×3), 127.4, 125.8 (C×2), 124.4, 120.3, 119.6, 118.2, 117.2, 61.3, 61.0, 45.0, 44.3, 43.0, 40.5, 39.4, 38.2, 36.3, 34.8, 33.4, 32.8, 31.6, 30.8, 30.5, 29.8 (C×2), 28.6, 27.9, 21.6, 18.6, 10.2. HRMS (ESI) calculated for $C_{42}H_{50}F_3O_6$ $[M + H]^+$ 707.3559, found 707.3553.

Compound **15**. Orange powder, 46% yield. M.p. 141.2-142.7 °C; ^{1}H NMR (300 MHz,

$CDCl_3$) δ_H: 0.57 (3H, s), 1.11 (3H, s), 1.20 (3H, s), 1.26 (3H, s), 1.44 (3H, s), 2.20 (3H, s), 3.89-3.95 (1H, m), 4.04-4.08 (1H, m), 4.24-4.28 (2H, m), 6.35 (1H, d, J = 7.2 Hz), 6.53 (1H, d, J = 16.0 Hz), 6.54 (1H, s), 7.01 (1H, d, J = 7.1 Hz), 7.65 (4H, m), 7.71 (1H, d, J = 16.0 Hz); ^{13}C NMR (75 MHz, $CDCl_3$) δ_C: 178.3 ,178.2, 169.8, 166.3, 164.7, 146.0, 143.0, 137.8, 134.0, 128.2 (C×3), 127.4, 125.9, 125.8, 124.0, 120.6, 119.5, 118.2, 117.1, 64.3, 64.0, 45.0, 44.3, 42.9, 40.4, 39.4, 38.2, 36.3, 34.8, 33.5, 32.8, 31.6, 30.8, 30.5, 29.8, 29.7, 28.6, 25.5, 25.2, 21.6, 18.5, 10.2. HRMS (ESI) calculated for $C_{43}H_{52}F_3O_6$ $[M + H]^+$ 721.3716, found 721.3724.

Compound **16**. Orange powder, 47% yield. M.p. 135.7-137.9 °C; ^{1}H NMR (300 MHz, $CDCl_3$) δ_H: 0.56 (3H, s), 1.10 (3H, s), 1.22 (3H, s), 1.25 (3H, s), 1.43 (3H, s), 2.19 (3H, s), 4.11-4.15 (1H, m), 4.32-4.39 (1H, m), 4.50-4.51 (2H, m), 6.28 (1H, d, J = 7.0 Hz), 6.52 (1H, s), 6.94 (1H, d, J = 6.9 Hz), 7.56 (2H, m), 8.02 (3H, m), 8.27 (1H, s); ^{13}C NMR (75 MHz, $CDCl_3$) δ_C: 178.3 ,178.1, 169.9, 164.7, 162.2, 155.7, 146.0, 134.1, 133.6, 131.4, 131.3 (C×2), 129.3 (C×2), 127.4, 119.5, 118.1, 117.1, 115.1, 102.3, 63.8, 61.7, 45.0, 44.2, 42.9, 40.5, 39.4, 38.2, 36.3, 34.8, 33.5, 32.7, 31.6, 30.9, 30.5, 29.7 (C×2), 28.6, 21.6, 18.7, 10.2. HRMS (ESI) calculated for $C_{41}H_{48}NO_6$ $[M + H]^+$ 650.3482, found 650.3478.

Compound **17**. Orange powder, 46% yield. M.p. 132.7-134.8 °C; ^{1}H NMR (300 MHz, $CDCl_3$) δ_H: 0.59 (3H, s), 1.12 (3H, s), 1.22 (3H, s), 1.28 (3H, s), 1.46 (3H, s), 2.20 (3H, s), 4.03-4.16 (2H, m), 4.34-4.48 (2H, m), 6.36 (1H, d, J = 7.1 Hz), 6.55 (1H, s), 7.01 (1H, d, J = 7.1 Hz), 7.55 (3H, m), 7.98 (2H, d, J = 7.9 Hz), 8.25 (1H, s).; ^{13}C NMR (75 MHz, $CDCl_3$) δ_C: 178.3 ,178.2, 169.7, 164.7, 162.5, 155.5, 146.0, 134.0,

133.5, 131.4, 131.1 (C×2), 129.3 (C×2), 127.4, 119.6, 118.2, 117.1, 115.3, 102.3, 63.2, 60.8, 45.0, 44.3, 42.9, 40.5, 39.4, 38.2, 36.4, 34.8, 33.4, 32.8, 31.6, 30.8, 30.5, 29.8 (C×2), 28.6, 27.7, 21.7, 18.5, 10.2. HRMS (ESI) calculated for $C_{42}H_{50}NO_6$ $[M + H]^+$ 664.3638, found 664.3640.

Compound **18**. Orange powder, 55% yield. M.p. 136.9-138.5 °C; ^{1}H NMR (300 MHz, $CDCl_3$) δ_H: 0.57 (3H, s), 1.11 (3H, s), 1.21 (3H, s), 1.30 (3H, s), 1.45 (3H, s), 2.21 (3H, s), 3.90-3.96 (1H, m), 4.04-4.15 (1H, m), 4.35-4.39 (2H, m), 6.36 (1H, d, J = 7.2 Hz), 6.56 (1H, s), 7.02 (1H, d, J = 7.1 Hz), 7.55 (3H, m), 8.02 (2H, d, J = 7.8 Hz), 8.30 (1H, s); ^{13}C NMR (75 MHz, $CDCl_3$) δ_C: 178.4 ,178.2, 169.9, 164.7, 162.4, 155.4, 146.0, 134.1, 133.4, 131.5, 131.2 (C×2), 129.3 (C×2), 127.4, 119.6, 118.2, 117.1, 115.1, 102.4, 66.1, 63.8, 45.0, 44.3, 42.9, 40.4, 39.4, 38.2, 36.4, 34.8, 33.5, 32.8, 31.6, 30.8, 30.6, 29.8, 29.7, 28.6, 25.4, 25.0, 21.6, 18.5, 10.3. HRMS (ESI) calculated for $C_{43}H_{52}NO_6$ $[M + H]^+$ 678.3795, found 678.3790.

Compound **19**. Orange powder, 48% yield. M.p. 141.1-142.5 °C; ^{1}H NMR (300 MHz, $CDCl_3$) δ_H: 0.57 (3H, s), 1.11 (3H, s), 1.23 (3H, s), 1.26 (3H, s), 1.44 (3H, s), 2.20 (3H, s), 2.47 (3H, s), 4.11-4.17 (1H, m), 4.32-4.40 (1H, m), 4.50-4.53 (2H, m), 6.28 (1H, d, J = 7.1 Hz), 6.53 (1H, s), 6.95 (1H, d, J = 7.1 Hz), 7.34 (2H, d, J = 7.9 Hz), 7.94 (2H, d, J = 7.8 Hz), 8.23 (1H, s); ^{13}C NMR (75 MHz, $CDCl_3$) δ_C: 178.3 ,178.2, 169.8, 164.7, 162.5, 155.6, 146.0, 145.0, 134.0, 131.5 (C×2), 130.1 (C×2), 128.8, 127.4, 119.6, 118.1, 117.0, 115.4, 100.9, 63.6, 61.8, 45.0, 44.2, 42.9, 40.5, 39.4, 38.2, 36.3, 34.8, 33.5, 32.7, 31.6, 30.9, 30.5, 29.7 (C×2), 28.6, 21.9, 21.6, 18.7, 10.2. HRMS (ESI) calculated for $C_{42}H_{50}NO_6$ $[M + H]^+$ 664.3638, found 664.3640.

Compound **20**. Orange powder, 51% yield. M.p. 137.5-139.3 °C; ^{1}H NMR (300 MHz, $CDCl_3$) δ_H: 0.58 (3H, s), 1.12 (3H, s), 1.21 (3H, s), 1.28 (3H, s), 1.46 (3H, s), 2.19 (3H, s), 2.46 (3H, s), 4.02-4.16 (2H, m), 4.32-4.38 (2H, m), 6.35 (1H, d, *J* = 7.1 Hz), 6.54 (1H, s), 7.00 (1H, d, *J* = 6.9 Hz), 7.31 (2H, d, *J* = 8.0 Hz), 7.89 (2H, d, *J* = 7.9 Hz), 8.20 (1H, s); ^{13}C NMR (75 MHz, $CDCl_3$) δ_C: 178.3 ,178.1, 169.7, 164.7, 162.6, 155.4, 146.0, 144.8, 134.0, 131.3 (C×2), 130.0 (C×2), 128.8, 127.4, 119.6, 118.2, 117.0, 115.7, 101.1, 63.0, 60.8, 45.0, 44.3, 42.9, 40.5, 39.4, 38.2, 36.4, 34.9, 33.4, 32.8, 31.6, 30.8, 30.5, 29.8 (C×2), 28.6, 27.8, 21.9, 21.7, 18.5, 10.2; ESI/HRMS (m/z) $[M+H]^+$ 574.1497. HRMS (ESI) calculated for $C_{43}H_{52}NO_6$ $[M + H]^+$ 678.3795, found 678.3788.

Compound **21**. Orange powder, 49% yield. M.p. 129-132.2 °C; ^{1}H NMR (300 MHz, $CDCl_3$) δ_H: 0.57 (3H, s), 1.11 (3H, s), 1.21 (3H, s), 1.27 (3H, s), 1.45 (3H, s), 2.21 (3H, s), 2.45 (3H, s), 3.88-3.95 (1H, m), 4.03-4.11 (1H, m), 4.33-4.37 (2H, m), 6.36 (1H, d, *J* = 7.2 Hz), 6.56 (1H, s), 7.02 (1H, d, *J* = 7.0 Hz), 7.32 (2H, d, *J* = 8.0 Hz), 7.93 (2H, d, *J* = 8.0 Hz), 8.25 (1H, s); ^{13}C NMR (75 MHz, $CDCl_3$) δ_C: 178.4 ,178.2, 169.9, 164.7, 162.7, 155.3, 146.0, 144.8, 134.1, 131.3 (C×2), 130.1 (C×2), 128.9, 127.4, 119.6, 118.2, 117.1, 115.7, 101.3, 65.9, 63.8, 45.0, 44.3, 42.9, 40.4, 39.4, 38.2, 36.4, 34.7, 33.5, 32.8, 31.6, 30.8, 30.6, 29.8, 29.7, 28.6, 25.5, 25.0, 21.9, 21.6, 18.5, 10.2. HRMS (ESI) calculated for $C_{44}H_{54}NO_6$ $[M + H]^+$ 692.3951, found 692.3944.

Compound **22**. Orange powder, 47% yield. M.p. 131.7-132.8 °C; ^{1}H NMR (300 MHz, $CDCl_3$) δ_H: 0.56 (3H, s), 1.11 (3H, s), 1.20 (3H, s), 1.26 (3H, s), 1.43 (3H, s), 2.16 (3H, s), 3.88 (3H, s), 4.08-4.13 (2H, m), 4.35-4.48 (2H, m), 6.34 (1H, d, *J* = 7.1 Hz),

6.52 (1H, s), 6.95 (3H, m), 7.63 (2H, d, J = 9.0 Hz), 8.17 (1H, s); ^{13}C NMR (75 MHz, $CDCl_3$) δ_C: 78.3 ,178.1, 170.0, 164.7, 161.1, 160.6, 153.7, 146.0, 134.0, 131.2 (C×2), 127.4, 126.3, 126.2, 119.5, 118.2, 117.2, 114.5 (C×2), 103.8, 64.2, 61.5, 56.1, 45.0, 44.2, 42.9, 40.5, 39.4, 38.2, 36.3, 34.8, 33.5, 32.7, 31.6, 30.9, 30.5, 29.8, 29.7, 28.6, 21.6, 18.7, 10.2. HRMS (ESI) calculated for $C_{42}H_{50}NO_7$ $[M + H]^+$ 680.3587, found 680.3591.

Compound **23**. Orange powder, 55% yield. M.p. 136.4-138.9 °C; ^{1}H NMR (300 MHz, $CDCl_3$) δ_H: 0.58 (3H, s), 1.12 (3H, s), 1.21 (3H, s), 1.28 (3H, s), 1.46 (3H, s), 2.19 (3H, s), 3.92 (3H, s), 4.01-4.16 (2H, m), 4.31-4.45 (2H, m), 6.36 (1H, d, J = 7.1 Hz), 6.54 (1H, s), 7.00 (1H, d, J = 7.0 Hz), 7.02 (2H, d, J = 8.8 Hz), 7.99 (2H, d, J = 8.8 Hz), 8.15 (1H, s); ^{13}C NMR (75 MHz, $CDCl_3$) δ_C: 178.3 ,178.1, 169.0, 164.7, 161.6, 160.3, 154.5, 146.0, 134.1, 131.1 (C×2), 127.4, 126.2 (C×2), 119.6, 118.2, 117.2, 114.6 (C×2), 105.3, 63.5, 60.7, 56.8, 45.0, 44.3, 42.9, 40.5, 39.4, 38.2, 36.3, 34.8, 33.4, 32.8, 31.6, 30.8, 30.5, 29.8, 29.7, 28.6, 27.7, 21.6, 18.6, 10.22. HRMS (ESI) calculated for $C_{43}H_{52}NO_7$ $[M + H]^+$ 694.3744, found 694.3742.

Compound **24**. Orange powder, 54% yield. M.p. 139.2-140.5 °C; ^{1}H NMR (300 MHz, $CDCl_3$) δ_H: 0.57 (3H, s), 1.11 (3H, s), 1.21 (3H, s), 1.27 (3H, s), 1.45 (3H, s), 2.21 (3H, s), 3.91 (3H, s), 4.03-4.10 (2H, m), 4.32-4.40 (2H, m), 6.36 (1H, d, J = 7.1 Hz), 6.56 (1H, s), 7.01 (1H, d, J = 7.0 Hz), 7.02 (2H, m), 8.04 (2H, m), 8.21 (1H, s).; ^{13}C NMR (75 MHz, $CDCl_3$) δ_C: 178.4 ,178.2, 170.0, 164.7, 163.9, 160.3, 154.7, 146.0, 134.1, 133.7 (C×2), 127.4, 124.5, 124.4, 119.6, 119.1, 118.2, 116.1, 114.8 (C×2), 102.3, 65.8, 63.8, 55.6, 45.1, 44.3, 43.0, 40.4, 39.5, 38.2, 36.4, 34.8, 33.5, 32.8, 31.5,

30.8, 30.6, 29.8, 29.7, 28.7, 25.5, 25.0, 21.6, 18.5, 10.2. HRMS (ESI) calculated for $C_{44}H_{54}NO_7$ $[M + H]^+$ 708.3900, found 708.3891.

Compound **25**. Orange powder, 47% yield. M.p. 138.4-139.7 °C; ^{1}H NMR (300 MHz, $CDCl_3$) δ_H: 0.58 (3H, s), 1.11 (3H, s), 1.23 (3H, s), 1.27 (3H, s), 1.45 (3H, s), 2.21 (3H, s), 4.13-4.17 (1H, m), 4.33-4.40 (1H, m), 4.49-4.54 (2H, m), 6.31 (1H, d, J = 7.2 Hz), 6.52 (1H, s), 6.98 (1H, d, J = 7.0 Hz), 7.24 (2H, t, J = 8.4 Hz), 8.08 (2H, dd, J = 8.5 Hz), 8.24 (1H, s); ^{13}C NMR (75 MHz, $CDCl_3$) δ_C: 178.3 ,178.1, 169.8, 164.7, 162.1, 161.3, 154.2, 146.0, 133.9 (C×2), 133.8, 127.8, 127.4, 119.6, 118.1, 117.1, 116.9, 116.6, 115.1, 102.1, 63.9, 61.6, 45.0, 44.2, 42.9, 40.5, 39.4, 38.2, 36.3, 34.8, 33.5, 32.7, 31.6, 30.9, 30.5, 29.8, 29.7, 28.6, 21.6, 18.7, 10.2. HRMS (ESI) calculated for $C_{41}H_{47}FNO_6$ $[M + H]^+$ 668.3387, found 668.3391.

Compound **26**. Orange powder, 49% yield. M.p. 129.4-131.0 °C; ^{1}H NMR (300 MHz, $CDCl_3$) δ_H: 0.59 (3H, s), 1.12 (3H, s), 1.22 (3H, s), 1.28 (3H, s), 1.46 (3H, s), 2.19 (3H, s), 4.02-4.17 (2H, m), 4.30-4.50 (2H, m), 6.36 (1H, d, J = 7.2 Hz), 6.54 (1H, s), 7.01 (1H, d, J = 7.1 Hz), 7.21 (2H, t, J = 8.6 Hz), 8.03 (2H, d, J = 8.8 Hz), 8.20 (1H, s); ^{13}C NMR (75 MHz, $CDCl_3$) δ_C: 178.4 ,178.2, 169.8, 164.7, 162.3, 161.3, 153.9, 146.0, 134.1, 133.8, 133.6, 127.8, 127.5, 119.6, 118.2, 117.1, 116.9, 116.7, 115.3, 103.5, 63.2, 60.8, 45.0, 44.3, 42.9, 40.5, 39.4, 38.2, 36.3, 34.8, 33.4, 32.8, 31.6, 30.8, 30.5, 29.8 (C×2), 28.6, 27.7, 21.7, 18.5, 10.2. HRMS (ESI) calculated for $C_{42}H_{49}FNO_6$ $[M + H]^+$ 682.3544, found 682.3544.

Compound **27**. Orange powder, 50% yield. M.p. 135.7-137.8 °C; ^{1}H NMR (300 MHz, $CDCl_3$) δ_H: 0.58 (3H, s), 1.12 (3H, s), 1.21 (3H, s), 1.28 (3H, s), 1.46 (3H, s), 2.19

(3H, s), 4.00-4.17 (2H, m), 4.30-4.50 (2H, m), 6.36 (1H, d, J = 7.1 Hz), 6.54 (1H, s), 7.02 (1H, d, J = 7.1 Hz), 7.21 (2H, t, J = 8.7 Hz), 8.03 (2H, d, J = 8.7 Hz), 8.20 (1H, s); ^{13}C NMR (75 MHz, $CDCl_3$) δ_C: 178.3 ,178.2, 169.9, 164.7, 162.2, 161.3, 154.5, 146.0, 134.0, 133.9, 133.7, 127.7, 127.4, 119.6, 118.2, 117.2, 116.9, 116.7, 115.2, 103.2, 64.3, 64.0, 45.0, 44.2, 42.9, 40.4, 39.4, 38.2, 36.3, 34.8, 33.5, 32.8, 31.6, 30.8, 30.5, 29.8, 29.7, 28.6, 25.5, 25.2, 21.6, 18.5, 10.2. HRMS (ESI) calculated for $C_{43}H_{51}FNO_6$ $[M + H]^+$ 696.3700, found 696.3709.

Compound **28**. Orange powder, 51% yield. M.p. 136.1-138.4 °C; ^{1}H NMR (300 MHz, $CDCl_3$) δ_H: 0.58 (3H, s), 1.11 (3H, s), 1.24 (3H, s), 1.27 (3H, s), 1.45 (3H, s), 2.21 (3H, s), 4.13-4.20 (1H, m), 4.34-4.42 (1H, m), 4.53-4.62 (2H, m), 6.32 (1H, d, J = 7.1 Hz), 6.53 (1H, s), 6.98 (1H, d, J = 7.0 Hz), 7.80 (2H, d, J = 8.3 Hz), 8.13 (2H, d, J = 8.2 Hz), 8.31 (1H, s); ^{13}C NMR (75 MHz, $CDCl_3$) δ_C: 178.3 ,178.1, 169.8, 164.7, 162.1, 153.6, 146.0, 135.3, 133.9, 131.2 (C×2), 129.1, 127.8, 126.3, 126.2, 125.5, 119.6, 118.1, 117.1, 114.5, 106.2, 64.2, 61.5, 45.0, 44.2, 42.9, 40.5, 39.4, 38.2, 36.3, 34.8, 33.6, 32.7, 31.6, 30.9, 30.5, 29.8, 29.7, 28.6, 21.6, 18.7, 10.2. HRMS (ESI) calculated for $C_{42}H_{47}F_3NO_6$ $[M + H]^+$ 718.3355, found 718.3364.

Compound **29**. Orange powder, 47% yield. M.p. 135.6-136.4 °C; ^{1}H NMR (300 MHz, $CDCl_3$) δ_H: 0.59 (3H, s), 1.12 (3H, s), 1.22 (3H, s), 1.30 (3H, s), 1.46 (3H, s), 2.18 (3H, s), 4.03-4.15 (2H, m), 4.34-4.50 (2H, m), 6.36 (1H, d, J = 7.2 Hz), 6.54 (1H, s), 7.02 (1H, d, J = 7.0 Hz), 7.77 (2H, d, J = 8.3 Hz), 8.07 (2H, d, J = 8.4 Hz), 8.27 (1H, s); ^{13}C NMR (75 MHz, $CDCl_3$) δ_C: 178.3 ,178.1, 170.0, 164.7, 161.7, 153.5, 146.0, 135.1, 134.2, 131.1 (C×2), 129.1, 127.4, 126.2 (C×2), 124.7, 119.6, 118.2, 117.6,

116.7, 105.5, 63.5, 60.7, 45.1, 44.3, 43.0, 40.5, 39.4, 38.2, 36.3, 34.8, 33.4, 32.8, 31.6, 30.8, 30.5, 29.8, 29.7, 28.6, 27.7, 21.6, 18.6, 10.2. HRMS (ESI) calculated for $C_{43}H_{49}F_3NO_6$ $[M + H]^+$ 732.3512, found 732.3513.

Compound **30**. Orange powder, 51% yield. M.p. 138.4-139.8 °C; ^{1}H NMR (300 MHz, $CDCl_3$) δ_H: 0.55 (3H, s), 1.08 (3H, s), 1.18 (3H, s), 1.24 (3H, s), 1.42 (3H, s), 2.16 (3H, s), 3.18-4.12 (2H, m), 4.27-4.42 (2H, m), 6.34 (1H, d, J = 7.1 Hz), 6.52 (1H, s), 6.91 (1H, d, J = 7.1 Hz), 7.71 (2H, d, J = 8.8 Hz), 8.07 (2H, d, J = 8.8 Hz), 8.40 (1H, s); ^{13}C NMR (75 MHz, $CDCl_3$) δ_C: 178.3 ,178.1, 170.0, 164.7, 161.8, 153.4, 146.0, 135.2, 134.2, 131.5 (C×2), 130.7, 127.5, 126.4 (C×2), 125.5, 119.5, 118.2, 117.2, 116.3, 105.2, 63.9, 61.8, 45.0, 44.2 42.9, 40.5, 39.4, 38.3, 36.3, 34.7, 33.5, 32.8, 31.6, 30.8, 30.5, 29.7 (C×2), 28.6, 25.4, 25.1, 21.6, 18.5, 10.3. HRMS (ESI) calculated for $C_{44}H_{51}F_3NO_6$ $[M + H]^+$ 746.3668, found 746.3656.

Compound **31**. Orange powder, 55% yield. M.p. 143.3-145.1 °C; ^{1}H NMR (300 MHz, $CDCl_3$) δ_H: 0.57 (3H, s), 1.11 (3H, s), 1.21 (3H, s), 1.30 (3H, s), 1.43 (3H, s), 2.21 (3H, s), 4.10-4.17 (1H, m), 4.31-4.39 (1H, m), 4.44-4.56 (2H, m), 6.28 (1H, d, J = 7.1 Hz), 6.51 (1H, s), 6.88 (1H, s), 6.97 (1H, d, J = 7.1 Hz), 7.53 (3H, m), 7.76 (2H, m); ^{13}C NMR (75 MHz, $CDCl_3$) δ_C: 178.3 ,178.1, 169.8, 164.6, 162.8, 146.0, 134.0, 133.9, 131.9, 129.4 (C×2), 128.4, 127.4, 127.1 (C×2), 127.0, 119.5, 118.1, 117.1, 114.8, 62.9, 61.9, 45.0, 44.2, 42.9, 40.5, 39.4, 38.2, 36.3, 34.8, 33.5, 32.8, 31.6, 30.9, 30.5, 29.7, 29.6, 28.6, 21.6, 18.7, 10.3. HRMS (ESI) calculated for $C_{41}H_{48}NO_6$ $[M + H]^+$ 650.3482, found 650.3485.

Compound **32**. Orange powder, 54% yield. M.p. 133.9-136.7 °C; ^{1}H NMR (300 MHz,

$CDCl_3$) δ_H: 0.58 (3H, s), 1.12 (3H, s), 1.22 (3H, s), 1.30 (3H, s), 1.46 (3H, s), 2.18 (3H, s), 4.02-4.18 (2H, m), 4.32-4.45 (2H, m), 6.36 (1H, d, J = 7.3 Hz), 6.54 (1H, s), 6.86 (1H, s), 7.00 (1H, d, J = 7.1 Hz), 7.49 (3H, m), 7.69 (2H, d, J = 7.9 Hz); ^{13}C NMR (75 MHz, $CDCl_3$) δ_C: 178.3 ,178.2, 169.8, 164.7, 163.1, 146.0, 134.1, 133.5, 131.7, 129.3 (C×2), 129.2, 128.8, 127.4, 127.0 (C×2), 119.5, 118.2, 117.1, 116.8, 62.3, 60.8, 45.1, 44.3, 43.0, 40.5, 39.4, 38.2, 36.3, 34.8, 33.4, 32.8, 31.6, 30.8, 30.5, 29.8, 29.7, 28.6, 27.6, 21.7, 18.6, 10.2. HRMS (ESI) calculated for $C_{42}H_{50}NO_6$ $[M + H]^+$ 664.3638, found 664.3641.

Compound **33**. Orange powder, 52% yield. M.p. 143.4-145.7 °C; ^{1}H NMR (300 MHz, $CDCl_3$) δ_H: 0.57 (3H, s), 1.12 (3H, s), 1.21 (3H, s), 1.27 (3H, s), 1.45 (3H, s), 2.22 (3H, s), 3.89-3.97 (1H, m), 4.05-4.13 (2H, m), 4.26-4.29 (1H, m), 6.36 (1H, d, J = 6.8 Hz), 6.55 (1H, s), 6.92 (1H, s), 7.04 (1H, d, J = 7.0 Hz), 7.50 (3H, m), 7.75 (2H, m); ^{13}C NMR (75 MHz, $CDCl_3$) δ_C: 178.3 ,178.2, 169.9, 164.7, 163.0, 146.0, 134.1, 133.6, 131.7, 129.4 (C×2), 129.1, 128.6, 127.4, 127.0 (C×2), 119.4, 118.2, 117.1, 116.4, 62.8, 60.8, 45.0, 44.3, 42.9, 40.5, 39.4, 38.2, 36.3, 34.8, 33.4, 32.8, 31.6, 30.8, 30.5, 29.8, 29.7, 28.7, 25.5, 25.0, 21.6, 18.6, 10.3HRMS (ESI) calculated for $C_{43}H_{52}NO_6$ $[M + H]^+$ 678.3795, found 678.3788.

Compound **34**. Orange powder, 53% yield. M.p. 136.9-138.2 °C; ^{1}H NMR (300 MHz, $CDCl_3$) δ_H: 0.57 (3H, s), 1.11 (3H, s), 1.21 (3H, s), 1.30 (3H, s), 1.44 (3H, s), 2.21 (3H, s), 2.44 (3H, s), 4.08-4.15 (1H, m), 4.31-4.38 (1H, m), 4.46-4.52 (2H, m), 6.29 (1H, d, J = 7.2 Hz), 6.51 (1H,), 6.83 (1H, s), 6.97 (1H, d, J = 7.1 Hz), 7.31 (2H, d, J = 8.0 Hz), 7.65 (2H, d, J = 8.0 Hz); ^{13}C NMR (75 MHz, $CDCl_3$) δ_C: 178.3 ,178.1, 169.7,

164.6, 163.0, 146.0, 142.7, 133.9, 130.1 (C×2), 129.0, 127.9, 127.4, 127.0 (C×2), 126.9, 119.5, 118.1, 117.1, 114.9, 62.8, 61.9, 45.0, 44.2, 42.9, 40.5, 39.4, 38.2, 36.3, 34.8, 33.6, 32.7, 31.6, 30.9, 30.5, 29.7, 29.6, 28.7, 21.6, 21.4, 18.6, 10.2. HRMS (ESI) calculated for $C_{42}H_{50}NO_6$ $[M + H]^+$ 664.3638, found 664.3643.

Compound **35**. Orange powder, 49% yield. M.p. 143.3-145.7 °C; ^{1}H NMR (300 MHz, $CDCl_3$) δ_H: 0.58 (3H, s), 1.12 (3H, s), 1.22 (3H, s), 1.28 (3H, s), 1.46 (3H, s), 2.17 (3H, s), 2.24 (3H, s), 4.02-4.17 (2H, m), 4.28-4.36 (2H, m), 6.36 (1H, d, J = 7.0 Hz), 6.54 (1H, s), 6.81 (1H, s), 6.99 (1H, d, J = 7.1 Hz), 7.27 (2H, d, J = 8.2 Hz), 7.59 (2H, d, J = 8.2 Hz); ^{13}C NMR (75 MHz, $CDCl_3$) δ_C: 178.3 ,178.2, 169.9, 164.7, 163.3, 146.0, 142.6, 134.0, 130.1 (C×2), 129.1, 127.9, 127.4, 127.0 (C×2), 126.5, 119.5, 118.2, 117.2, 115.0, 64.1, 63.0, 45.0, 44.2, 42.9, 40.4, 39.4, 38.2, 36.4, 34.8, 33.5, 32.8, 31.6, 30.8, 30.5, 29.8, 29.7, 28.7, 27.6, 21.6, 21.4, 18.6, 10.2. HRMS (ESI) calculated for $C_{43}H_{52}NO_6$ $[M + H]^+$ 678.3795, found 678.3793.

Compound **36**. Orange powder, 55% yield. M.p. 141.7-142.8 °C; ^{1}H NMR (300 MHz, $CDCl_3$) δ_H: 0.56 (3H, s), 1.11 (3H, s), 1.20 (3H, s), 1.27 (3H, s), 1.44 (3H, s), 2.21 (3H, s), 2.42 (3H, s), 3.88-3.94 (1H, m), 4.04-4.09 (1H, m), 4.31-4.35 (2H, m), 6.36 (1H, d, J = 7.2 Hz), 6.53 (1H, s), 6.88 (1H, s), 7.02 (1H, d, J = 7.3 Hz), 7.28 (2H, d, J = 8.0 Hz), 7.64 (2H, d, J = 8.1 Hz); ^{13}C NMR (75 MHz, $CDCl_3$) δ_C: 178.3 ,178.2, 170.0, 164.7, 163.4, 146.0, 142.4, 134.1, 130.0 (C×2), 129.1, 127.9, 127.4, 127.0 (C×2), 126.2, 119.5, 118.2, 117.2, 115.1, 65.2, 63.9, 45.0, 44.3, 42.9, 40.4, 39.4, 38.2, 36.3, 34.8, 33.5, 32.8, 31.6, 30.8, 30.5, 29.8, 29.7, 28.6, 25.4, 25.1, 21.6, 21.4, 18.5, 10.2 HRMS (ESI) calculated for $C_{44}H_{54}NO_6$ $[M + H]^+$ 692.3951, found 692.3943.

Compound **37**. Orange powder, 52% yield. M.p. 137.3-139.5 °C; ^{1}H NMR (300 MHz, $CDCl_3$) δ_H: 0.57 (3H, s), 1.11 (3H, s), 1.21 (3H, s), 1.26 (3H, s), 1.44 (3H, s), 2.21 (3H, s), 3.89 (3H, s), 4.08-4.15 (1H, m), 4.30-4.38 (1H, m), 4.45-4.51 (2H, m), 6.29 (1H, d, J = 7.2 Hz), 6.51 (1H, s), 6.75 (1H, s), 6.98 (1H, d, J = 7.2 Hz), 7.01 (2H, d, J = 8.9 Hz), 7.72 (2H, d, J = 9.0 Hz); ^{13}C NMR (75 MHz, $CDCl_3$) δ_C: 178.3 ,178.1, 169.9, 164.6, 163.1, 162.6, 146.0, 133.9, 131.0, 128.9 (C×2), 127.4, 126.4, 125.3, 119.5, 118.1, 117.8, 117.1, 114.8 (C×2), 62.7, 62.0, 55.6, 45.0, 44.2, 42.9, 40.5, 39.4, 38.2, 36.3, 34.8, 33.6, 32.8, 31.6, 30.8, 30.5, 29.7 (C×2), 28.6, 21.6, 18.6, 10.2. HRMS (ESI) calculated for $C_{42}H_{50}NO_7$ $[M + H]^+$ 680.3587, found 680.3589.

Compound **38**. Orange powder, 51% yield. M.p. 134.8-136.5 °C; ^{1}H NMR (300 MHz, $CDCl_3$) δ_H: 0.57 (3H, s), 1.12 (3H, s), 1.21 (3H, s), 1.27 (3H, s), 1.44 (3H, s), 2.17 (3H, s), 3.89 (3H, s), 3.99-4.19 (2H, m), 4.26-4.45 (2H, m), 6.35 (1H, d, J = 7.1 Hz), 6.53 (1H, s), 6.72 (1H, s), 6.96 (2H, d, J = 8.9 Hz), 6.99 (1H, d, J = 7.0 Hz), 7.64 (2H, d, J = 8.9 Hz); ^{13}C NMR (75 MHz, $CDCl_3$) δ_C: 178.3 (C×2), 169.8, 164.7, 163.8, 163.2, 146.0, 134.1, 130.0 (C×2), 129.0, 127.5, 127.0, 125.0, 119.5, 118.1, 117.8, 117.1, 114.9 (C×2), 62.2, 60.8, 54.7, 45.1, 44.3, 42.9, 40.5, 39.4, 38.2, 36.3, 34.8, 33.4, 32.8, 31.6, 30.8, 30.5, 29.8, 29.7, 28.6, 27.6, 21.7, 18.6, 10.2. HRMS (ESI) calculated for $C_{43}H_{52}NO_7$ $[M + H]^+$ 694.3744, found 694.3746.

Compound **39**. Orange powder, 53% yield. M.p. 139.7-141.3 °C; ^{1}H NMR (300 MHz, $CDCl_3$) δ_H: 0.57 (3H, s), 1.11 (3H, s), 1.21 (3H, s), 1.27 (3H, s), 1.44 (3H, s), 2.22 (3H, s), 3.89 (3H, s), 3.89-3.92 (1H, m), 4.04-4.08 (1H, m), 4.31-4.33 (2H, m), 6.36 (1H, d, J = 6.8 Hz), 6.54 (1H, s), 6.81 (1H, s), 6.98 (2H, d, J = 8.5 Hz), 7.03 (1H, d, J

= 7.1 Hz), 7.71 (2H, d, *J* = 8.3 Hz); ^{13}C NMR (75 MHz, $CDCl_3$) δ_C: 178.3, 178.2, 169.9, 164.9, 163.6, 163.0, 146.0, 134.0, 130.3, 128.8 (C×2), 127.3, 126.2, 124.5, 119.5, 118.1, 117.7, 117.0, 114.7 (C×2), 65.1, 63.9, 55.5, 45.0, 44.3, 43.0, 40.4, 39.4, 38.2, 36.4, 34.8, 33.5, 32.8, 31.6, 30.8, 30.6, 29.8, 29.7, 28.7, 25.4, 25.2, 21.7, 18.5, 10.2. HRMS (ESI) calculated for $C_{44}H_{54}NO_7$ $[M + H]^+$ 708.3900, found 708.3903.

Compound **40**. Orange powder, 54% yield. M.p. 136.8-138.3 °C; ^{1}H NMR (300 MHz, $CDCl_3$) δ_H: 0.57 (3H, s), 1.11 (3H, s), 1.22 (3H, s), 1.27 (3H, s), 1.44 (3H, s), 2.22 (3H, s), 4.11-4.17 (1H, m), 4.32-4.38 (1H, m), 4.44-4.54 (2H, m), 6.32 (1H, d, *J* = 6.8 Hz), 6.51 (1H, s), 6.82 (1H, s), 7.00 (1H, d, *J* = 6.6 Hz), 7.22 (2H, t, *J* = 8.4 Hz), 7.77 (2H, m); ^{13}C NMR (75 MHz, $CDCl_3$) δ_C: 178.3, 178.2, 169.9, 166.4, 164.7, 163.0, 146.0, 134.1 (C×2), 129.3, 129.2, 128.7, 127.3, 125.3, 119.5, 118.2, 117.1, 116.8, 116.5, 114.9, 63.4, 61.7, 45.0, 44.2, 42.9, 40.4, 39.4, 38.2, 36.3, 34.8, 33.4, 32.8, 31.6, 30.8, 30.5, 29.8, 29.7, 28.6, 27.6, 21.6, 18.5, 10.3. HRMS (ESI) calculated for $C_{41}H_{47}FNO_6$ $[M + H]^+$ 668.3387, found 668.3387.

Compound **41**. Orange powder, 49% yield. M.p. 129.0-131.9 °C; ^{1}H NMR (300 MHz, $CDCl_3$) δ_H: 0.56 (3H, s), 1.11 (3H, s), 1.20 (3H, s), 1.27 (3H, s), 1.44 (3H, s), 2.17 (3H, s), 4.01-4.16 (2H, m), 4.30-4.44 (2H, m), 6.34 (1H, d, *J* = 7.2 Hz), 6.52 (1H, s), 6.78 (1H, s), 7.00 (1H, d, *J* = 7.1 Hz), 7.16 (2H, t, *J* = 8.4 Hz), 7.68 (2H, m); ^{13}C NMR (75 MHz, $CDCl_3$) δ_C: 178.3, 178.2, 169.8, 166.4, 164.7, 163.0, 146.0, 134.1 (C×2), 129.3, 129.2, 128.5, 127.3, 125.3, 119.5, 118.2, 117.1, 116.8, 116.5, 114.9, 62.4, 60.7, 45.1, 44.2, 42.9, 40.8, 39.4, 38.2, 36.3, 34.8, 33.4, 32.8, 31.6, 30.8, 30.5, 29.8, 29.7, 28.6, 27.6, 21.7, 18.6, 10.2. HRMS (ESI) calculated for $C_{42}H_{49}FNO_6$ [M +

H]$^+$ 682.3544, found 682.3544.

Compound **42**. Orange powder, 48% yield. M.p. 131.2-133.4 ^{o}C; ^{1}H NMR (300 MHz, $CDCl_3$) δ_H: 0.57 (3H, s), 1.12 (3H, s), 1.20 (3H, s), 1.27 (3H, s), 1.45 (3H, s), 2.22 (3H, s), 3.89-3.95 (1H, m), 4.04-4.10 (1H, m), 4.32-4.36 (2H, m), 6.36 (1H, d, J = 7.2 Hz), 6.53 (1H, s), 6.87 (1H, s), 7.02 (1H, d, J = 7.0 Hz), 7.18 (2H, t, J = 8.3 Hz), 7.76 (2H, m); ^{13}C NMR (75 MHz, $CDCl_3$) δ_C: 178.3 (C×2), 169.9, 166.6, 164.8, 163.1, 146.0, 134.0 (C×2), 129.3, 129.2, 128.9, 127.3, 125.3, 119.5, 118.2, 117.1, 116.8, 116.5, 114.9, 65.4, 63.9, 45.0, 44.3, 42.9, 40.4, 39.4, 38.2, 36.3, 34.8, 33.5, 32.8, 31.6, 30.8, 30.5, 29.8, 29.7, 28.6, 25.4, 25.1, 21.6, 18.5, 10.2. HRMS (ESI) calculated for $C_{43}H_{51}FNO_6$ [M + H]$^+$ 696.3700, found 696.3698.

Compound **43**. Orange powder, 47% yield. M.p. 137.9-138.8 ^{o}C; ^{1}H NMR (300 MHz, $CDCl_3$) δ_H: 0.57 (3H, s), 1.12 (3H, s), 1.22 (3H, s), 1.28 (3H, s), 1.45 (3H, s), 2.23 (3H, s), 4.10-4.18 (1H, m), 4.35-4.39 (1H, m), 4.49-4.52 (2H, m), 6.34 (1H, d, J = 7.1 Hz), 6.55 (1H, s), 6.95 (1H, s), 7.03 (1H, d, J = 6.9 Hz), 7.79 (2H, d, J = 8.1 Hz), 7.88 (2H, d, J = 8.1 Hz); ^{13}C NMR (75 MHz, $CDCl_3$) δ_C: 178.3, 178.0, 169.7, 164.6, 162.3, 146.1, 135.1, 133.8, 130.7 (C×2), 127.3 (C×2), 126.4 (C×2), 125.5, 124.5, 119.5, 118.1, 117.1, 114.3, 63.3, 61.8, 45.0, 44.2, 42.9, 40.5, 39.4, 38.2, 36.3, 34.8, 33.6, 32.7, 31.5, 30.8, 30.5, 29.7 (C×2), 28.6, 21.6, 18.7, 10.2. HRMS (ESI) calculated for $C_{42}H_{47}F_3NO_6$ [M + H]$^+$ 718.3355, found 718.3361.

Compound **44**. Orange powder, 49% yield. M.p. 133.3-135.6 ^{o}C; ^{1}H NMR (300 MHz, $CDCl_3$) δ_H: 0.57 (3H, s), 1.12 (3H, s), 1.21 (3H, s), 1.28 (3H, s), 1.45 (3H, s), 2.17 (3H, s), 4.02-4.17 (2H, m), 4.33-4.47 (2H, m), 6.36 (1H, d, J = 7.1 Hz), 6.52 (1H, s),

6.92 (1H, s), 7.01 (1H, d, J = 7.1 Hz), 7.74 (2H, d, J = 8. 5Hz), 7.80 (2H, d, J = 8.3 Hz); ^{13}C NMR (75 MHz, $CDCl_3$) δ_C: 178.2, 178.1, 169.8, 164.7, 162.6, 146.0, 135.4, 134.0, 131.0 (C×2), 127.5 (C×2), 127.2, 126.4, 126.3, 125.1, 124.2, 119.5, 118.2, 117.1, 114.5, 62.7, 60.7, 45.0, 44.3, 42.9, 40.5, 39.4, 38.2, 36.3, 34.8, 33.4, 32.8, 31.6, 30.8, 30.5, 29.8, 29.7, 28.6, 27.6, 21.6, 18.6, 10.2. HRMS (ESI) calculated for $C_{43}H_{49}F_3NO_6$ $[M + H]^+$ 732.3512, found 732.3507.

Compound **45**. Orange powder, 50% yield. M.p. 142.1-143.7 °C; ^{1}H NMR (300 MHz, $CDCl_3$) δ_H: 0.57 (3H, s), 1.12 (3H, s), 1.21 (3H, s), 1.27 (3H, s), 1.46 (3H, s), 2.22 (3H, s), 3.89-3.97 (1H, m), 4.05-4.13 (1H, m), 4.34-4.38 (2H, m), 6.37 (1H, d, J = 7.0 Hz), 6.54 (1H, s), 7.01 (1H, s), 7.04 (1H, d, J = 7.0 Hz), 7.76 (2H, d, J = 8.3 Hz), 7.88 (2H, d, J = 8.3 Hz); ^{13}C NMR (75 MHz, $CDCl_3$) δ_C: 178.3, 178.2, 170.18, 164.6, 162.8, 146.0, 140.2, 135.2, 134.2, 131.5 (C×2), 127.5 (C×2), 127.2, 126.4, 126.3, 124.8, 124.3, 119.5, 118.2, 117.4, 114.6, 65.6, 63.9, 45.0, 44.3, 42.9, 40.4, 39.4, 38.2, 36.3, 34.8, 33.5, 32.8, 31.6, 30.8, 30.5, 29.8, 29.7, 28.6, 25.4, 25.1, 21.6, 18.5, 10.2. HRMS (ESI) calculated for $C_{44}H_{50}F_3NO_6$ $[M + H]^+$ 746.3668, found 746.3663.

Compound **46**. Orange powder, 49% yield. M.p. 142.5-143.6 °C; ^{1}H NMR (300 MHz, $CDCl_3$) δ_H: 0.56 (3H, s), 1.12 (3H, s), 1.22 (3H, s), 1.27 (3H, s), 1.44 (3H, s), 2.21 (3H, s), 4.48 (2H, m), 4.81 (2H, m), 5.93 (2H,s), 6.35 (1H, d, J = 7.4 Hz), 6.53 (1H, s), 6.95 (1H, s), 7.01 (1H, d, J = 6.8 Hz), 7.19 (3H, m), 7.76 (2H, m); ^{13}C NMR (75 MHz, $CDCl_3$) δ_C: 178.3, 177.8, 170.1, 164.7, 162.9, 146.0, 134.1 (C×2), 131.7, 129.4 (C×2), 129.2, 128.8, 127.4, 127.1 (C×2), 126.8, 126.6, 119.5, 118.2, 117.2, 115.0, 65.1, 63.7, 45.0, 44.2, 42.9, 40.5, 39.4, 38.3, 36.3, 34.7, 33.5, 32.8, 31.6, 30.9, 30.6, 29.8, 29.6,

28.6, 21.6, 18.6, 10.3. HRMS (ESI) calculated for $C_{43}H_{50}NO_6$ $[M + H]^+$ 676.3638, found 676.3633.

Compound **47**. Orange powder, 48% yield. M.p. 139.4-142.1 °C; ^{1}H NMR (300 MHz, $CDCl_3$) δ_H: 0.56 (3H, s), 1.12 (3H, s), 1.22 (3H, s), 1.27 (3H, s), 1.44 (3H, s), 2.21 (3H, s), 3.89 (3H, s), 4.47 (2H, m), 4.79 (2H, m), 5.92 (2H,s), 6.36 (1H, d, J = 7.1 Hz), 6.53 (1H, s), 6.83 (1H, s), 6.98 (2H, d, J = 9.0 Hz), 7.02 (1H, d, J = 7.0 Hz), 7.72 (2H, d, J = 8.9 Hz); ^{13}C NMR (75 MHz, $CDCl_3$) δ_C: 178.3, 177.9, 170.1, 164.8, 162.5, 160.3, 146.0, 134.1, 129.0, 128.9 (C×2), 127.9, 127.4, 126.8, 126.1, 125.8, 119.5, 118.2, 117.9, 117.2, 114.7 (C×2), 64.9, 63.7, 55.6, 45.1, 44.2, 42.9, 40.5, 39.4, 38.3, 36.3, 34.7, 33.5, 32.8, 31.6, 30.9, 30.6, 29.8, 29.6, 28.6, 21.6, 18.6, 10.3 HRMS (ESI) calculated for $C_{44}H_{52}NO_7$ $[M + H]^+$ 706.3744, found 706.3744.

Compound **48**. Orange powder, 54% yield. M.p. 138.6-140.1 °C; ^{1}H NMR (300 MHz, $CDCl_3$) δ_H: 0.56 (3H, s), 1.12 (3H, s), 1.22 (3H, s), 1.28 (3H, s), 1.45 (3H, s), 2.22 (3H, s), 4.48 (2H, m), 4.81 (2H, m), 5.92 (2H,s), 6.37 (1H, d, J = 7.1 Hz), 6.54 (1H, s), 6.90 (1H, s), 7.04 (1H, d, J = 7.1 Hz), 7.19 (2H, t, J = 8.6 Hz), 7.77 (2H, m).; ^{13}C NMR (75 MHz, $CDCl_3$) δ_C: 178.3, 177.8, 169.9, 166.4, 164.9, 162.8, 146.0, 134.3 (C×2), 129.4, 129.3, 129.1, 128.6, 127.4, 126.6, 125.5, 119.4, 118.2, 117.1, 116.8, 116.5, 114.9, 65.2, 63.7, 45.1, 44.2, 43.0, 40.5, 39.4, 38.2, 36.3, 34.7, 33.5, 32.8, 31.6, 30.8, 30.6, 29.8, 29.6, 28.6, 21.6, 18.6, 10.3 HRMS (ESI) calculated for $C_{43}H_{49}FNO_6$ $[M + H]^+$ 694.3538, found 694.3554.

(9) Procedures for the Preparation of Compound 41-Bio. A mixture of **11a** (1.0 eq), 3-bromo-1-propanol (1.1 eq) and K_2CO_3 (5.0 eq) in acetone was refluxed

overnight and evaporated. The crude product was purified by column chromatography [PE/EA = 2:1 to 1:1 (v/v)] to afford **11b**. **11b** (1 eq), **8a** (1 eq) and K_2CO_3 (3 eq) were dissolved in MeOH. The reaction was reluxed at 70°C for 6 h. The reaction mixture was washed by EtOAc (×2). Then the water layer was acidified using 1 M hydrochloric acid solution to pH = 4 and filtered. The filter cake was the crude product **11c**. **11c** (1 eq), 1,3-dibromopropane (1 eq) and K_2CO_3 (3 eq) were added in acetone and this reaction mixture was refluxed overnight. Then the solution was evaporated. The crude product was purified by column chromatography [PE/EA = 2:1 (v/v)] to afford **11d**. **11d** (1 eq), Biotin (2 eq), DCC (1 eq) and DMAP (5 mg) were reacted in DMF at 30°C for 24h.The reaction was washed with CH_2Cl_2 (100 ml) for four times. The combined organic layers were washed by aqueous saturated NaCl solution (30 ml), and then dried over sodium sulfate, filtered, and the solvent was evaporated. The crude product was purified by column chromatography [DCM:MeOH = 20:1 to 10:1 (v:v)] to afford **11e**. **41-Bio** were synthesized using **11e** and CEL by the methods of **1-48**. The crude product was purified by column chromatography [DCM:MeOH = 20:1 to 10:1 (v:v)] to afford **41-Bio**.

Compound **41-Bio**. Orange powder, 10% yield. M.p. 138.6-140.1 °C; ^{1}H NMR (300 MHz, $CDCl_3$) δ_H: 0.57 (3H, s), 0.91 (3H, s), 1.12 (3H, s), 1.27 (3H, s), 1.45 (3H, s), 2.16 (3H, s), 4.12-4.32 (10H, m), 6.37 (1H, d, J = 7.2 Hz), 6.53 (1H, s), 6.72 (1H, s),6.94 (3H, m), 7.53 (1H, dd, *J* = 3.3, 5.5 Hz), 7.60 (1H, br s), 7.64 (1H, br s), 7.72 (1H, dd, *J* = 3.3, 5.5 Hz); ^{13}C NMR (75 MHz, $CDCl_3$) δ_C: 178.4, 178.2, 173.5, 169.7, 164.7, 163.4, 161.7, 146.1, 134.0, 130.9, 128.8, 125.9, 124.3, 119.6, 118.2, 117.2,

115.3, 114.5, 68.2, 64.8, 62.1, 60.9, 60.8, 60.2, 55.3, 44.5, 40.5, 38.8, 38.2, 36.4, 35.0, 33.9, 32.9,31.6, 30.9, 30.4, 28.6, 27.7,24.8, 23.8, 21.7, 18.6, 14.1, 10.2. HRMS (ESI) calculated for $C_{55}H_{69}N_3O_{10}S$ $[M + H]^+$ 964.4782, found 964.4779.

(10) Procedures for the Preparation of Compound 41-H. A mixture of **41** (1.0 eq) and Methyl thioglycolate (1.1 eq) in MeOH was stirred for 15 min. The reaction mixture was concentrated under vacuum and the residue was dissolved in CH_2Cl_2. Then the crude product and acetic anhydride (1 ml) was added in pyridine. The mixture reacted in room temperature for 12 h. Then the reaction mixture was suspended in CH_2Cl_2 and washed by water (×2). Then the organic layer was washed by aqueous saturated $CuSO_4$ and NaCl solution (30 ml), and then dried over sodium sulfate, filtered, and the solvent was evaporated. The crude product was purified by column chromatography [PE/EA = 3:1-1.5:1 (v/v)] to afford **41-H**.

Compound **41-H**. Colorless powder, 54% yield. M.p. 132.6-133.7 ^oC; ^1H NMR (300 MHz, $CDCl_3$) δ_H: 0.58 (3H, s), 1.11 (3H, s), 1.20 (3H, s), 1.27 (3H, s), 1.60 (3H, s), 2.26 (6H, s), 2.32 (3H, s), 3.25 (1H, d, J = 14.7 Hz), 3.50 (1H, d, J = 14.7 Hz), 3.78 (3H, s), 4.03 (1H, m), 4.12 (1H, m), 4.38 (2H, m), 4.74 (1H, d, J = 6.03 Hz), 6.03 (1H, d, J = 6.0 Hz), 6.81 (1H, s), 7.16 (1H, dd, *J* = 5.0, 8.5 Hz), 7.72 (1H, dd, *J* = 5.0, 8.8 Hz); ^{13}C NMR (75 MHz, $CDCl_3$) δ_C: 178.2, 171.1, 168.3, 168.1, 166.3, 162.9, 153.5, 149.7, 141.8, 138.7, 129.7, 129.5, 129.3, 129.2, 128.8, 128.7, 118.2, 117.3, 116.7, 116.4, 114.8, 62.5, 60.8, 52.3, 45.3 (C×2), 44.6, 44.5, 38.3, 37.8, 36.6, 35.1, 34.8, 34.4, 32.9, 31.5, 30.6, 30.5, 30.2 (C×2), 29.8, 28.8, 27.7, 22.6, 22.1, 20.6, 20.3, 18.6, 11.9. , 173.5, 169.7, 164.7, 163.4, 161.7, 146.1, 134.0, 130.9, 128.8, 125.9, 124.3,

119.6, 118.2, 117.2, 115.3, 114.5, 68.2, 64.8, 62.1, 60.9, 60.8, 60.2, 55.3, 44.5, 40.5, 38.8, 38.2, 36.4, 35.0, 33.9, 32.9,31.6, 30.9, 30.4, 28.6, 27.7,24.8, 23.8, 21.7, 18.6, 14.1, 10. HRMS (ESI) calculated for $C_{49}H_{58}FNNaO_{10}S$ $[M + Na]^+$ 894.3663, found 894.3648.

(11) MTT Assay. All hybrids were evaluated for their inhibitory activities against A549, MCF-7, HOS and HepG2 by MTT method. Briefly, 100 μL of each cell (5.0×10^4 cells/ml) were seeded into 96-well plates and incubated for 24 h. Different concentrations of the drug were added into the 96-well plates. Respective concentrations of DMSO were used as control. Then these plates were incubated for 48 h. MTT solution (5 mg/ml) was added, and cultured (4 h). Supernatant was abandoned before adding 100 ml DMSO to each well. The OD at 570 nm was measured using a microplate reader (POLARstar Omega, Offenburg, Germany). Every assay was performed in triplicate. Data are presented as the mean ± SD (n = 3).

(12) ATP-Sepharose Binding Assay. The assay was described previously.[30] Total of 5 mg of human Hsp90α protein with DMSO, CEL or **41** (5/10 μM) were incubated on ice in 200 ml incubation buffer consisting of 10 mM Tris-HCl, 50 mM KCl, 5 mM $MgCl_2$, 2 mM DTT, 20 mM Na_2MoO_4, 0.01% Nonidet P-40, pH 7.5. After 30 min, 25 ml of pre-equilibrated γ-phosphate-linked ATP-sepharose (Jena Bioscience GmbH, Jena, Germany) was added to tubes, which were then incubated at 37 ^oC for another 30 min with frequent mixing to resuspend the resin. Following incubation, the sepharose was washed, pelleted and analyzed by SDS-PAGE.

(13) Immunoprecipitation. A549 cells were seeded (5×10^5 cells) in 6 cm dishes

and incubated with 24 h. DMSO and **41** was added to the dishes with 5 μM and then these dishes were incubated for 6 h. The cells were lysed and the proteins were extracted. Then Cdc37 was pulled down by Hsp90α-sepharose. Equal amounts of total protein were subjected to SDS-PAGE to evaluate the levels of the target proteins. The monoclonal antibodies were purchased (Abcam, Cambridge, UK).

(14) Western Blotting Analysis. A549 cells were seeded (5×10^5 cells) in 6 cm dishes and incubated for 12 h. Then these cells were incubated with DMSO/**41**/CEL with indicated concentrations for another 12 h. The cells were lysed and the proteins were extracted. Then the proteins were diluted to 3 mg/ml (BCA method). Each sample (10 μL) was analyzed by SDS-PAGE (10 % gel). Then the proteins were detected by the conventional method.

(15) 41-Bio pull down experiment. The recombinant Cdc37 protein (5 mg) were incubated with biotin for 2 h at 10 °C, or different concentrations of **41** for 2 h before or after incubated with **41-Bio** (0.5 μM) for 2 h at 10 °C. Then the protein was pulled down using streptavidin beads. The beads were washed with PBS (1% DMSO, including compound). The total proteins (input), bound proteins were immunoblotted.

(16) Thiol-binding experiment. 41 (0.02 mmol) with or without DTT (0.04 mmol) was dissolved in NMR tube using DMSO-d_6 (600 μl). Then ^{1}H NMR spectrum of the mixture was detected after reaction in ultrasound for 20 min.

(17) UV absorption experiment. 41 (100 μM) and GSH (100 μM) or Cdc37 (1.5 μM) or Hsp90 (1.5 μM) were dissolved in PBS (1% DMSO) respectively. Then the solution was incubated at 37 °C for 0, 5, 15 and 30 min. The UV spectrum of the

solution (200-500 nm) was monitored.

(18) Molecular Modeling. The X-ray structure of the human $Hsp90_N$-$Cdc37_M$ protein (2K5B) was used. The molecular docking software used in this study was Autodock Vina 1.1.2.[31] The parameters were set to "center x = 2.094; center y = 1.667; center z = -3.372; size x = 30; size y = 30; size z = 30".

The X-ray structure of the human $Cdc37_M$ protein (2W0G) was used.

(19) Mitochondrial Membrane Potential. A549 cells (4×10^5 cells) were incubated in 6 cm dish for 24 h. Then DMSO/**41** was added to the cells with indicated concentrations for 24 h. Cells were harvested at 2000 rpm for 5 min and then washed twice with ice-cold PBS, followed by resuspension in JC-1 (5 mg/mL) and incubation at 37 °C for 15 min. After the cells were rinsed three times and suspended in PBS, the JC-1 fluorescence was analysis by flow cytometry.

(20) Hoechst-33342&PI Staining. A549 cells (4×10^5 cells) were incubated in 6 cm dish for 24 h. Then A549 cells were treated with the DMSO/**41** at indicated concentrations for 48 h. Cells were washed twice by PBS. Then cells were incubated with Hoechst-33342 (10 μg/ml) and PI for 5 min at room temperature in the darkness. After incubation, stained cells were observed under a fluorescent microscope (CORPORATION, Japan).

(21) Cell Apoptosis Analysis. A549 cells (4×10^5 cells) were incubated in 6 cm dish for 24 h. Then DMSO/**41**/CEL was added to the cells with indicated concentrations. After another incubation of 48 h, the cells were harvested softly and washed twice with cold PBS (2000 *g* for 5 min). Then the cells were added to 250 μL binding buffer

containing 2.5 μL PI and 2.5 μL Annexin V (KeyGEN, China). The mixture was incubated at room temperature for 15 min in the darkness and analyzed by flow cytometry.

(22) Cell Cycle Analysis. A549 cells (4×10^5 cells) were incubated in 6 cm dishes for 24 h. Then DMSO/**41**/CEL was added to the dishes with different concentrations. After incubation of 24 h, the cells were harvested and washed twice with cold PBS. Then the cell was fixed in ethanol (75 %) at - 20 °C for at least 12 h. The cells were washed with buffer A to remove the ethanol. The cells were followed suspended in buffer A (250 μL) containing 250 mg/ml RNase A and cultured at 37 °C for 30 min. Finally, 2.5 μL propidium iodide (PI) (KeyGEN, China) was added and incubated at room temperature in dark for 15 min. The cells were analyzed by flow cytometry (BD Accuri C6 flow cytometer, Franklin Lakes, NJ).

ASSOCIATED CONTENT

Supporting Information

The Supporting Information is available free of charge on the ACS Publications website at DOI: .

Structural characterization of the compounds (^{1}H NMR, ^{13}C NMR, ESI/HRMS spectrum of the final compounds **1-48**, **41-H** and **41-Bio**); The synthetic route of compound **41-H**; HPLC analysis of target compounds; Molecular string files for all the final target compounds (CSV).

AUTHOR INFORMATION

Corresponding Authors

*For L.C.: phone, +86-25-83271447; Email, *chenli627@cpu.edu.cn*.

*For J.S.: phone, +86-25-83271447; E-mail, *sjbcpu@gmail.com.*

Author Contributions

[δ]*These authors contribute equally to this work.*

Notes

The authors declare no competing financial interest.

ACKNOWLEDGEMENTS

This work was financially supported by "Double First Class" Subject Innovation Team Construction Project of China Pharmaceutical University (CPU2018GY12) and College Students Innovation Project for the R&D of Novel Drugs (No. J1310032).

ABBREVIATIONS USED

Hsp90-Cdc37, heat shock protein 90-cell division cycle 37; CEL, celastrol; Cdc37, cycle 37; Hop homeodomain only protein; Akt, protein kinase B; Cdk4, cyclin-dependent kinases 4; Her-2, human epidermal growth factor receptor-2; c-Met, tyrosine-protein kinase Met; $Hsp90_N$, terminal domain of Hsp90; $Cdc37_{M,}$ the middle domain of Cdc37; CA, cinnamic acid; CDDO-Me, bardoxolone methyl; EDCI, 1-(3-dimethylaminopropyl)-3-ethylcarbodiimide hydrochloride; DMAP, dimethylaminopyridine; α-CN CA, α-cyano substituted cinnamic acids; β-CN CA, β-cyano substituted cinnamic acids; DMF, N,N-dimethylformamide; Bind P, bound proteins; GSH, Glutathione;PI, propidium iodide.

References

(1) Ferrarini, M.; Heltai, S.; Zocchi, M. R.; Rugarli, C. Unusual expression and

localization of heat-shock proteins in human tumor cells. Int. J. Cancer 1992, 51, 613-619.

(2) Kosano, H.; Stensgard, B.; Charlesworth, M. C.; McMahon, N.; Toft, D. The assembly of progesterone receptor-hsp90 complexes using purified proteins. J. Biol. Chem. 1998, 273, 32973-32979.

(3) Lee, P.; Rao, J.; Fliss, A.; Yang, E.; Garrett, S.; Caplan, A. J. The Cdc37 protein kinase-binding domain is sufficient for protein kinase activity and cell viability. J. Cell Biol. 2002, 159, 1051-1059.

(4) Pearl, L. H. Hsp90 and Cdc37 -- a chaperone cancer conspiracy. Curr. Opin. Genet. Dev. 2005, 15, 55-61.

(5) Calderwood, S. K. Cdc37 as a co-chaperone to Hsp90. Subcell. Biochem. 2015, 78, 103-112.

(6) Wang, L,; Li, L.; Gu, K.; Xu, X. L.; Sun, Y.; You, Q. D. Targeting Hsp90-Cdc37: a promising therapeutic strategy by inhibiting Hsp90 chaperone function. Curr. Drug Targets 2017, 18, 1572-1585.

(7) Zhou, Y. X.; Huang, Y. L. Antiangiogenic effect of celastrol on the growth of human glioma: An *in vitro* and *in vivo* study. Chin. Med. J. (Engl.) 2009, 122, 1666-1673.

(8) Jiang, H. L.; Jin, J. Z.; Wu, D.; Xu, D.; Lin, GF.; Yu, H.; Ma, D. Y.; Liang, J. Celastrol exerts synergistic effects with PHA-665752 and inhibits tumor growth of c-Met-deficient hepatocellular carcinoma *in vivo*. Mol. Biol. Rep. 2013, 40, 4203-4209.

(9) Yang, H.; Chen, D.; Cui, Q. C.; Yuan, X.; Dou, Q. P. Celastrol, a triterpene extracted from the Chinese "Thunder of God Vine," is a potent proteasome inhibitor and suppresses human prostate cancer growth in nude mice. Cancer Res. 2006, 66, 4758-4765.

(10) Sreeramulu, S.; Gande, S. L.; Göbel, M.; Schwalbe, H. Molecular mechanism of inhibition of the human protein complex Hsp90-Cdc37, a kinome chaperone-cochaperone, by Triterpene Celastrol. Angew. Chem. Int. Ed. 2009, 48, 5853-5855.

(11) Zhang, T.; Hamza, A.; Cao, X.; Wang, B.; Yu, S.; Zhan, C.; Sun, D. A novel Hsp90 inhibitor to disrupt Hsp90/Cdc37 complex against pancreatic cancer cells. Mol. Cancer Ther. 2008, 7, 162-170.

(12) Sreeramulu, S.; Jonker, H. R.; Langer, T.; Richter, C.; Lancaster, C. Roy D.; Schwalbe, H. The human Cdc37-Hsp90 complex studied by NMR. J. Biol. Chem. 2009, 6, 3885-3896.

(13) Xu, M.; Li, N.; Zhao, Z.; Shi, Z.; Sun, J.; Chen, L. Design, synthesis and antitumor evaluation of novel celastrol derivatives. Eur. J. Med. Chem. 2019, 174, 265-276.

(14) Jiang, F.; Wang, H. J.; Bao, Q. C.; Wang, L.; Jin, Y. H.; Zhang, Q.; Jiang, D.; You, Q. D.; Xu. X. L. Optimization and biological evaluation of celastrol derivatives as Hsp90-Cdc37 interaction disruptors with improved druglike properties. Bioorg Med. Chem. 2016, 24, 5431-5439.

(15) Sayama, M.; Inoue, A.; Nakamura, S.; Jung, S.; Ikubo, M.; Otani, Y.; Uwamizu,

A.; Kishi, T.; Makide, K.; Aoki, J.; Hirokawa, T.; Ohwada, T. Probing the hydrophobic binding pocket of G-protein-coupled lysophosphatidylserine receptor GPR34/LPS1 by docking-aided structure-activity analysis. J. Med. Chem. 2017, 60, 6384-6399.

(16) Giroud, M.; Harder, M.; Kuhn, B.; Haap, W.; Trapp, N.; Schweizer, W. B.; Schirmeister, T.; Diederich, F. Fluorine scan of inhibitors of the cysteine protease human cathepsin L: dipolar and quadrupolar effects in the π-stacking of fluorinated phenyl rings on peptide amide bonds. Chem. Med. Chem. 2016, 11, 1042-1047.

(17) De, P.; Baltas, M.; Bedos-Belval, F. Cinnamic acid derivatives as anticancer agents. Curr. Med. Chem. 2011, 18, 1672-1703.

(18) Liang, C.; Pei, S.; Ju, W.; Jia, M.; Tian, D.; Tang, Y.; Mao, G. Synthesis and in vitro and in vivo antitumour activity study of 11-hydroxyl esterified bergenin/cinnamic acid hybrids. Eur. J. Med. Chem. 2017, 133, 319-328.

(19) Xu, C. C.; Deng, T.; Fan, M. L.; Lv, W. B.; Liu, J. H.; Yu, B. Y. Synthesis and in vitro antitumor evaluation of dihydroartemisinin-cinnamic acid ester derivatives. Eur. J. Med. Chem. 2016, 107, 192-203.

(20) Guo, W. B.; Yan, M. M.; Xu, B.; Chu, F. H.; Wang, W.; Zhang, C. Z.; Jia, X. H.; Han, Y. T.; Xiang, H. J.; Zhang, Y. Z.; Wang, P. L.; Lei, H. M. Design, synthesis, and biological evaluation of the novel glycyrrhetinic acid-cinnamoyl hybrids as anti-tumor agents. Chem. Cent. J. 2016, 10, 11.

(21) Cai, X.; Jin, J.; He, M. H. Advances in structural modifications of celastrol. Arkivoc 2016, I, 172-182.

(22) Tang, K.; Huang, Q.; Zeng, J.; Wu, G.; Huang J.; Pan, J.; Lu W. Design, synthesis and biological evaluation of C(6)-modified celastrol derivatives as potential antitumor agents. Molecules 2014, 19, 10177-10188.

(23) Klaić, L.; Morimoto, R. I.; Silverman, R. B. Celastrol analogues as inducers of the heat shock response. Design and synthesis of affinity probes for the identification of protein targets. ACS Chem. Biol. 2012, 7, 928-937.

(24) Chen, L.; Shang, J.; Wang, Z. F.; Zhang, Y. H.; Tian, J. D. Synthesis and biological evaluation of nitrate-oleanolic acid hybrids as inhibitors of HepG2 cell apoptosis. Yao Xue Xue Bao 2010, 45, 1516-1522.

(25) Chen, L.; Zhang, Y. H.; Kong, X. W.; Peng, S. X.; Tian, J. Synthesis and biological evaluation of nitric oxide-releasing derivatives of oleanolic acid as inhibitors of HepG2 cell apoptosis. Bioorg. Med. Chem. Lett. 2007, 17, 2979-2982.

(26) Tambe, S., Blott, H.; Fülöp, A.; Spang, N.; Flottmann, D.; Bräse, S.; Hopf, C.; Junker, H. D. Structure-performance relationships of phenyl cinnamic acid derivatives as MALDI-MS matrices for sulfatide detection. Anal. Bioanal. Chem. 2017, 409, 1569-1580.

(27) Fryszkowska, A.; Fisher, K.; Gardiner, J. M.; Stephens, G. M. A short, chemoenzymatic route to chiral β-aryl-γ-amino acids using reductases from anaerobic bacteria. Org. Biomol. Chem. 2010, 8, 533-535.

(28) Schmidt, T. J.; Lyss, G.; Pahl, H. L.; Merfort, I. Helenanolide type sesquiterpene lactones. Part 5: the role of glutathione addition under physiological conditions. Bioorg. Med. Chem. 1999, 7, 2849-2855.

(29) Li, Y.; Zhang, T.; Schwartz, S. J.; Sun, D. New developments in Hsp90 inhibitors as anti-cancer therapeutics: mechanisms, clinical perspective and more potential. Drug Resist. Updat. 2009, 12, 17-27.

(30) Grenert. J. P.; Sullivan, W. P.; Fadden. P.; Haystead, T. A.; Clark, J,; Mimnaugh. E.; Krutzsch, H.; Ochel, H. J.; Schulte, T. W.; Sausville, E.; Neckers, L. M.; Toft, D. O. The amino-terminal domain of heat shock protein 90 (hsp90) that binds GA is an ATP/ADP switch domain that regulates hsp90 conformation. J. Biol. Chem. 1997, 272, 23843-23850.

(31) Trott, O.; Olson, A. J. AutoDock Vina: improving the speed and accuracy of docking with a new scoring function, efficient optimization and multithreading. J. Comput. Chem. 2010, 31, 455-461.

Figure captions

Figure 1. Comparison of inhibition rates of target compounds. (A) Inhibition rates of **1-45** and CEL at 1.5 μM in A549 cells. IR: inhibition rate. (B) The average inhibition rates of **31-45** classified by the different groups in benzene. (C) Inhibition rate of **31-45**. (D) Inhibition rate of **1-45** classified by lengths of linker.

Figure 2. Effects of **41** on the level of Hsp90-Cdc37 complex *in vitro*. (A) Effects of **41** on the binding of ATP and Hsp90. Purified Hsp90α was pulled down by γ-phosphate-linked ATP-Sepharose in the presence of **41** or CEL. Hsp90α was detected by Western blot. (B) Effects of **41** on the amount of Cdc37 associated with Hsp90. A549 cells were treated with DMSO or **41** for 6 h. Cell lysate were immunoprecipitated by Hsp90α antibody. Western blot was done for detection of Hsp90 and Cdc37. (C) Quantitative analysis of co-IP. Data were expressed as the

mean ± SD (n = 3). **$P < 0.01$ *vs.* DMSO group.

Figure 3. Effects of **41** and CEL on Hsp90-Cdc37clients. A549 cells were treated with DMSO, **41** and CEL for 12 h, and the relative levels of p-Akt and Cdk4 expression were determined by Western blot assays using Hsp90 as a control. Data are representative images and expressed as the means ± SD of each group of cells from three separate experiments. (A) Western blot analysis of the relative levels of p-AKT and Cdk4 expression. (B) Quantitative analysis. **$P < 0.01$ *vs.* the DMSO group.

Figure 4. 41-Bio binds to Cdc37. The recombinant Cdc37 protein (5 mg) were incubated with different concentrations of **41** for 2 h before or after incubated with **41-Bio** (0.5 μM) for 2 h, and then pulled down using streptavidin beads. The total proteins (input), bound proteins (Bind P) were immunoblotted. Data were expressed as the mean ± SD (n = 3).**$P < 0.01$ *vs.* **41** (0.5 μM) group.

Figure 5. Overlay of ^{1}H NMR spectrum of **41** with and without DL-Dithiothreitol (DTT) in DMSO-d_6. **41** (0.02 mmol) and DTT (0.04 mmol) were dissolved in DMSO-d_6. Then ^{1}H NMR spectrum of the mixture was detected after reaction in ultrasound for 20 min.

Figure 6. UV spectrum of **41** monitored after addition of GSH, Cdc37 and Hsp90. **41**(100 μM) and GSH (100 μM) or Cdc37 (1.5 μM) or Hsp90 (1.5 μM) were dissolved in PBS (1% DMSO) respectively. Then the solution was incubated at 37 ^{o}C for 0, 5, 15 and 30 min. The UV spectrum of the solution (200-500 nm) was monitored. (A) UV spectrum of **41** was monitored after incubation with GSH, Cdc37 and Hsp90. (B)

Analysis of the UV assay. A0, absorbance of the solution at 440 nm with 0 min. A, absorbance of the solution at 440 nm with the corresponding time. Data were expressed as the mean ± SD (n = 3).**$P < 0.01$ *vs.* 0 min group.

Figure 7. Molecular docking of **41** to $Hsp90_N$-$Cdc37_M$. (A) Chemical structure of **41**. (B) Binding mode of **41** with the $Hsp90_N$-$Cdc37_M$ complex (PDB ID 2K5B). The complex was shown in a cartoon representation. The side chain R166 (yellow), R167 (green) and W168 (purple) of $Cdc37_M$ and **41** (gray) were shown in a stick type. The expected hydrogen bonds were indicated by the dashed yellow lines.

Figure 8. Anti-proliferative activity of **41-H** in comparison with that of **41**, methyl thioglycolate and their mixture in A549 cells.

Figure 9. The structure of $Cdc37_M$ (PDB ID 2W0G). (A) The location of Cys183. (B) The location of Cys203.

Figure 10. Effects of **41** on clients of Hsp90-Cdc37 and apoptosis-related proteins in A549 cells. A549 cells were treated with DMSO or **41** for 12 h, and the relative levels of Hsp90, p-AKT, Cdk4, Bcl-2, Bax and Caspase-3 expression were determined by Western blot assays using β-actin as a control. Data are representative images and expressed as the means ± SD of each group of cells from three separate experiments. (A) Western blot analysis of the relative levels of Hsp90, p-Akt, Cdk4, Bcl-2, Bax and Caspase-3 expression. (B) Quantitative analysis. *$P < 0.05$, **$P < 0.01$, vs the DMSO-treated control group.

Figure 11. Effects on $\Delta\psi_m$ of **41** in A549 cells. A549 cells were treated with DMSO or **41** for 24 h and then analyzed by fluorescence microscopy and flow cytometry after

JC-1 staining. (A) Flow cytometry analysis of A549 cells treated with DMSO and **41**. (B) The quantification of cells (%) with red and green aggregates. The values are presented as mean ± SD (n = 3). $^{**}P < 0.01$ *vs.* the DMSO group.

Figure 12. The morphological apoptosis induced by **41** in A549. A549 cells were treated with **41** or DMSO for 48 h. Fluorescence microscopy images of A549 cells stained by Hoechst 33342 and propidium iodide (PI). The apoptotic cells were stained by Hoechst 33342 in bright blue and the dead cells were stained by PI in red.

Figure 13. Apoptotic effects of **41** and CEL in A549 cells. Treatment with DMSO or **41** or CEL for 48 h, A549 cells were collected and stained with Annexin V/PI, followed by flow cytometric analysis. (A) Flow cytometry analysis of A549 cells treated with DMSO, **41** and CEL. (B) Representative histograms for the numbers of living cells and apoptotic cells (%). The values were presented as the mean ± SD (n = 3). $^{**}P < 0.05$ *vs.* the DMSO group.

Figure 14. Effect of **41** on cell cycle progression of A549 cells. Treatment of A549 cells with DMSO and **41** (0.2, 0.4 and 0.8 μM) for 24 h, intracellular DNA was stained with PI. Cell cycle distribution was analyzed by flow cytometry. (A) Flow cytometry analysis of cell cycle distribution of **41** on A549. (B) The quantification of cells (%) in each cell phase. The values are presented as mean ± SD (n = 3). $^{*}P < 0.01$, $^{**}P < 0.05$ *vs.* the DMSO group.

Table of Contents graphic

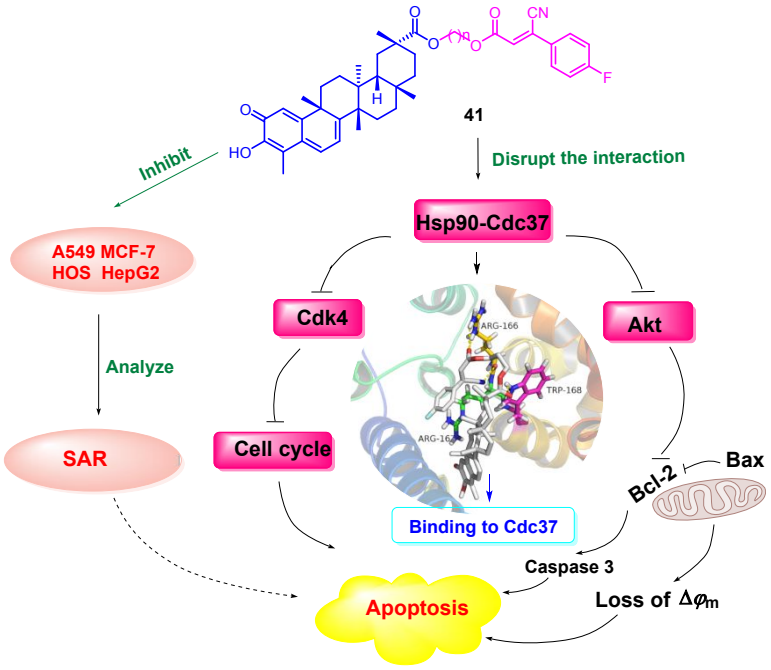

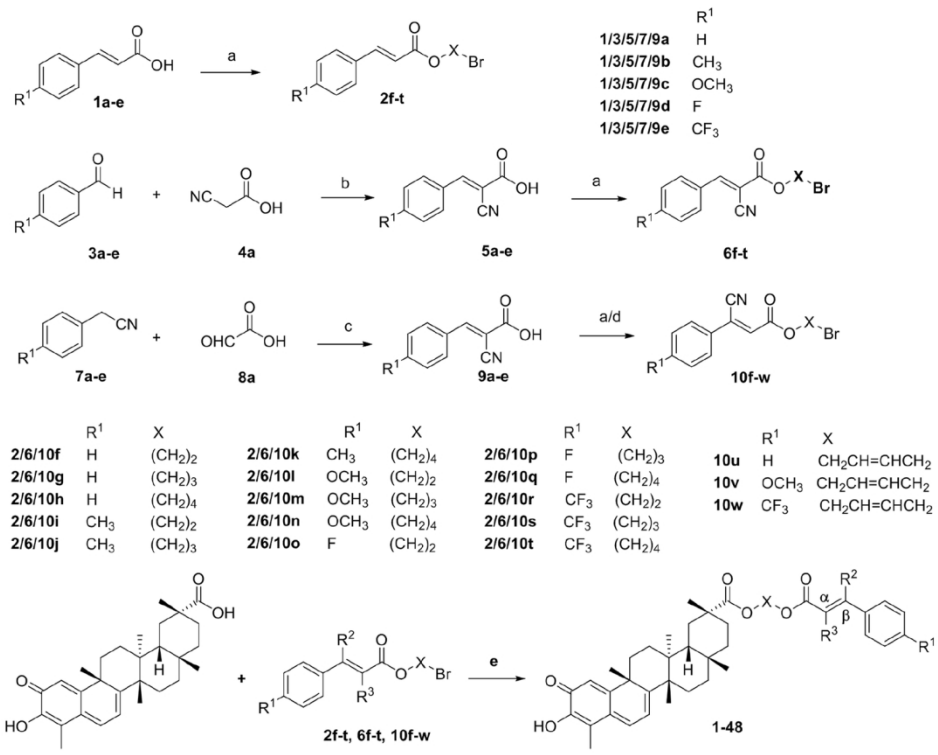

150x123mm (300 x 300 DPI)

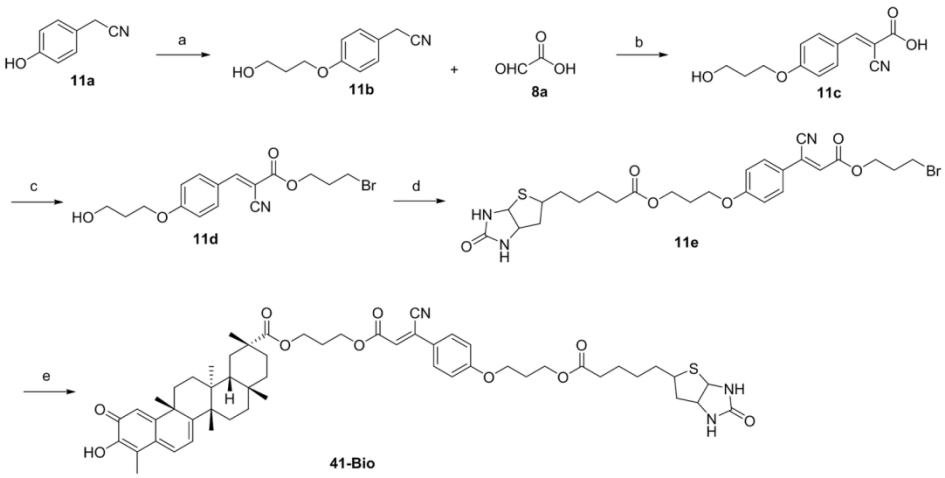

150x75mm (300 x 300 DPI)

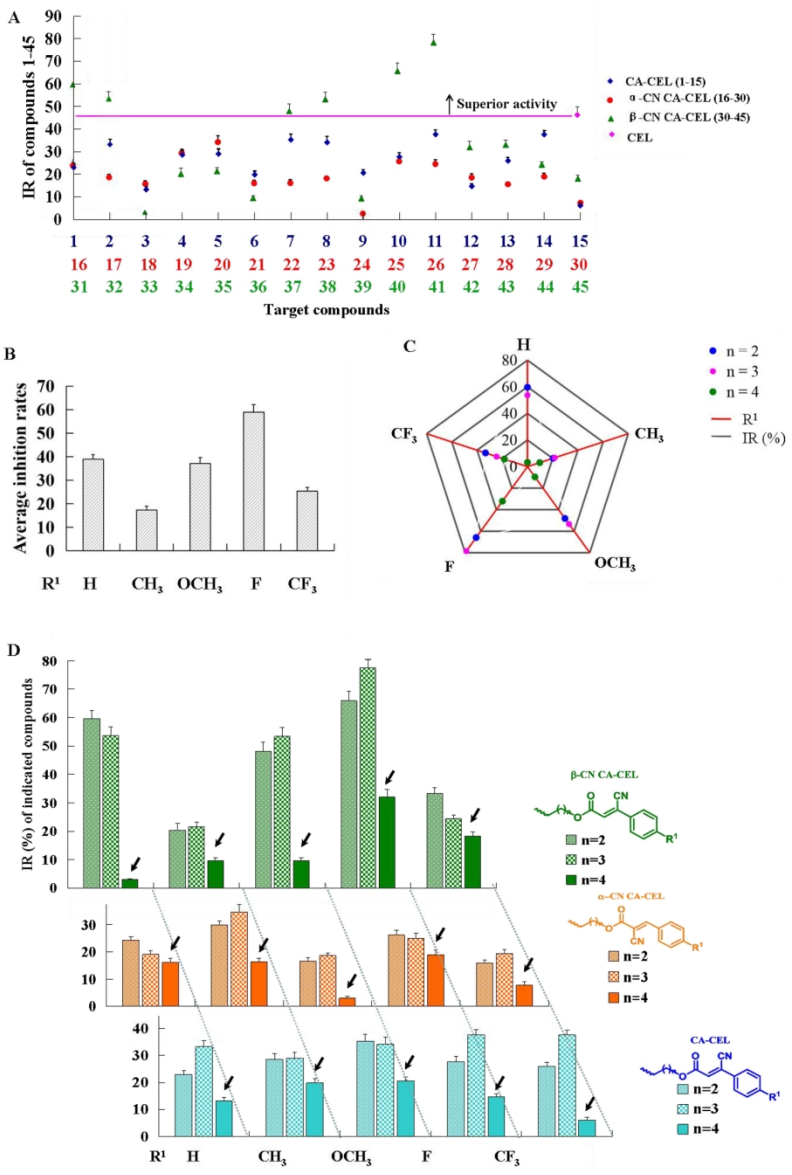

Figure 1. Comparison of inhibition rates of target compounds. (A) Inhibition rates of 1-45 and CEL at 1.5 μM in A549 cells. IR: inhibition rate. (B) The average inhibition rates of 31-45 classified by the different groups in benzene. (C) Inhibition rate of 31-45. (D) Inhibition rate of 1-45 classified by lengths of linker.

150x200mm (300 x 300 DPI)

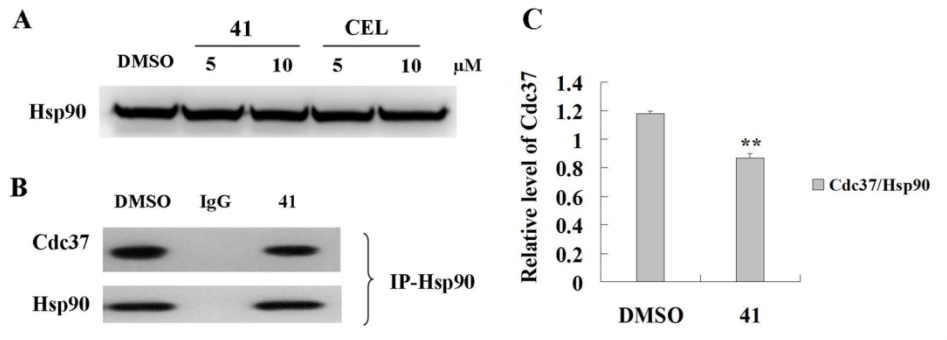

Figure 2. Effects of 41 on the level of Hsp90-Cdc37 complex in vitro. (A) Effects of 41 on the binding of ATP and Hsp90. Purified Hsp90α was pulled down by γ-phosphate-linked ATP-Sepharose in the presence of 41 or CEL. Hsp90α was detected by Western blot. (B) Effects of 41 on the amount of Cdc37 associated with Hsp90. A549 cells were treated with DMSO or 41 for 6 h. Cell lysate were immunoprecipitated by Hsp90α antibody. Western blot was done for detection of Hsp90 and Cdc37. (C) Quantitative analysis of co-IP. Data were expressed as the mean ± SD (n = 3). **P < 0.01 vs. DMSO group.

150x66mm (300 x 300 DPI)

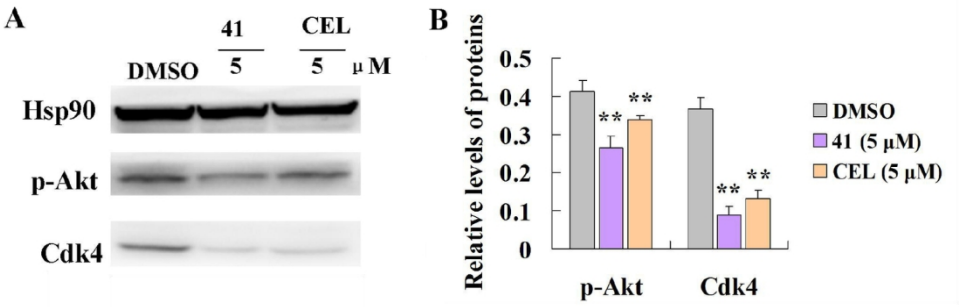

Figure 3. Effects of 41 and CEL on Hsp90-Cdc37clients. A549 cells were treated with DMSO, 41 and CEL for 12 h, and the relative levels of p-Akt and Cdk4 expression were determined by Western blot assays using Hsp90 as a control. Data are representative images and expressed as the means ± SD of each group of cells from three separate experiments. (A) Western blot analysis of the relative levels of p-AKT and Cdk4 expression. (B) Quantitative analysis. **P < 0.01 vs. the DMSO group.

150x49mm (300 x 300 DPI)

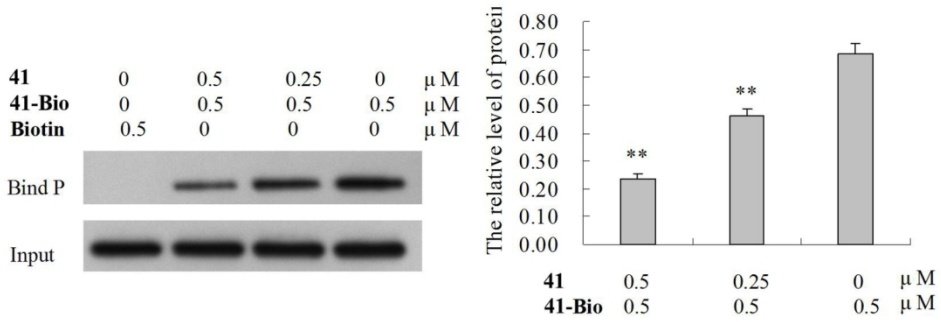

Figure 4. 41-Bio binds to Cdc37. The recombinant Cdc37 protein (5 mg) were incubated with different concentrations of 41 for 2 h before or after incubated with 41-Bio (0.5 μM) for 2 h, and then pulled down using streptavidin beads. The total proteins (input), bound proteins (Bind P) were immunoblotted. Data were expressed as the mean ± SD (n = 3).**P < 0.01 vs. 41 (0.5 μM) group.

150x54mm (300 x 300 DPI)

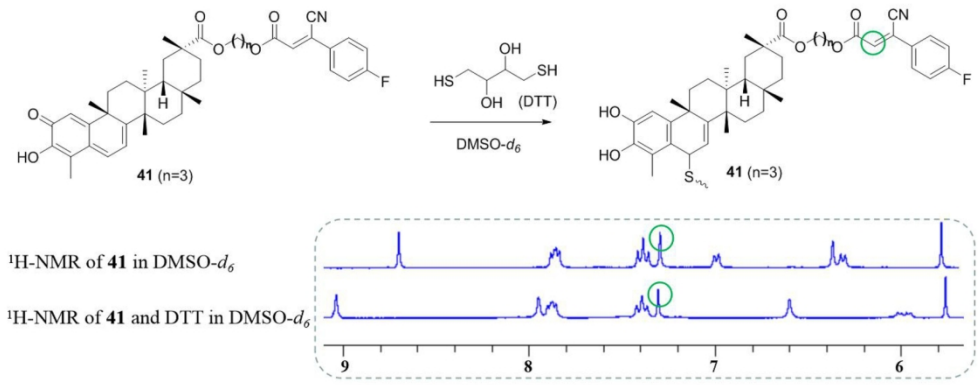

Figure 5. Overlay of 1H NMR spectrum of 41 with and without DL-Dithiothreitol (DTT) in DMSO-d6. 41 (0.02 mmol) and DTT (0.04 mmol) were dissolved in DMSO-d6. Then 1H NMR spectrum of the mixture was detected after reaction in ultrasound for 20 min.

150x63mm (300 x 300 DPI)

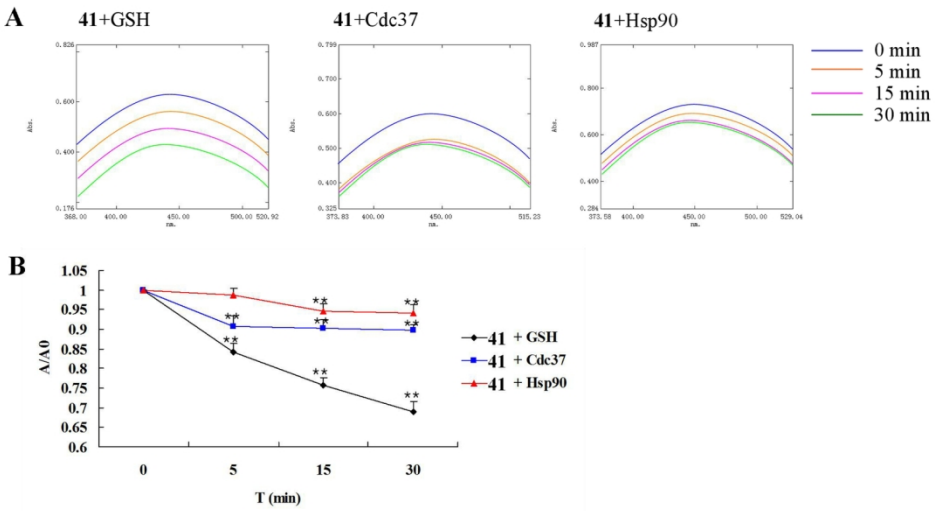

Figure 6. UV spectrum of 41 monitored after addition of GSH, Cdc37 and Hsp90. 41(100 μM) and GSH (100 μM) or Cdc37 (1.5 μM) or Hsp90 (1.5 μM) were dissolved in PBS (1% DMSO) respectively. Then the solution was incubated at 37 oC for 0, 5, 15 and 30 min. The UV spectrum of the solution (200-500 nm) was monitored. (A) UV spectrum of 41 was monitored after incubation with GSH, Cdc37 and Hsp90. (B) Analysis of the UV assay. A0, absorbance of the solution at 440 nm with 0 min. A, absorbance of the solution at 440 nm with the corresponding time. Data were expressed as the mean ± SD (n = 3).**P < 0.01 vs. 0 min group.

149x78mm (300 x 300 DPI)

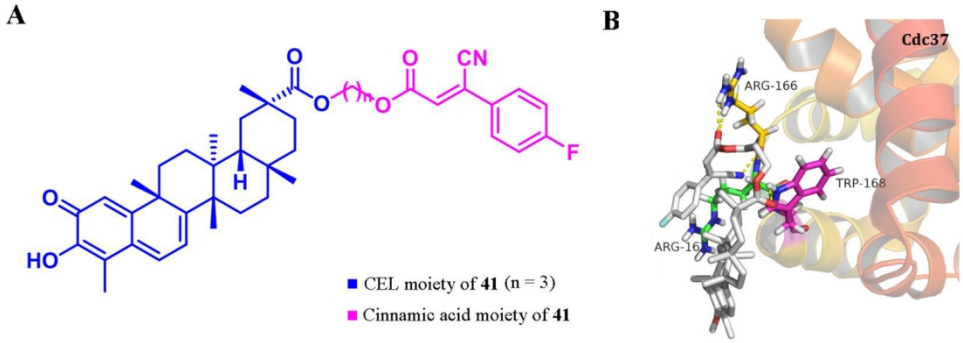

Figure 7. Molecular docking of 41 to Hsp90N-Cdc37M. (A) Chemical structure of 41. (B) Binding mode of 41 with the Hsp90N-Cdc37M complex (PDB ID 2K5B). The complex was shown in a cartoon representation. The side chain R166 (yellow), R167 (green) and W168 (purple) of Cdc37M and 41 (gray) were shown in a stick type. The expected hydrogen bonds were indicated by the dashed yellow lines.

134x48mm (300 x 300 DPI)

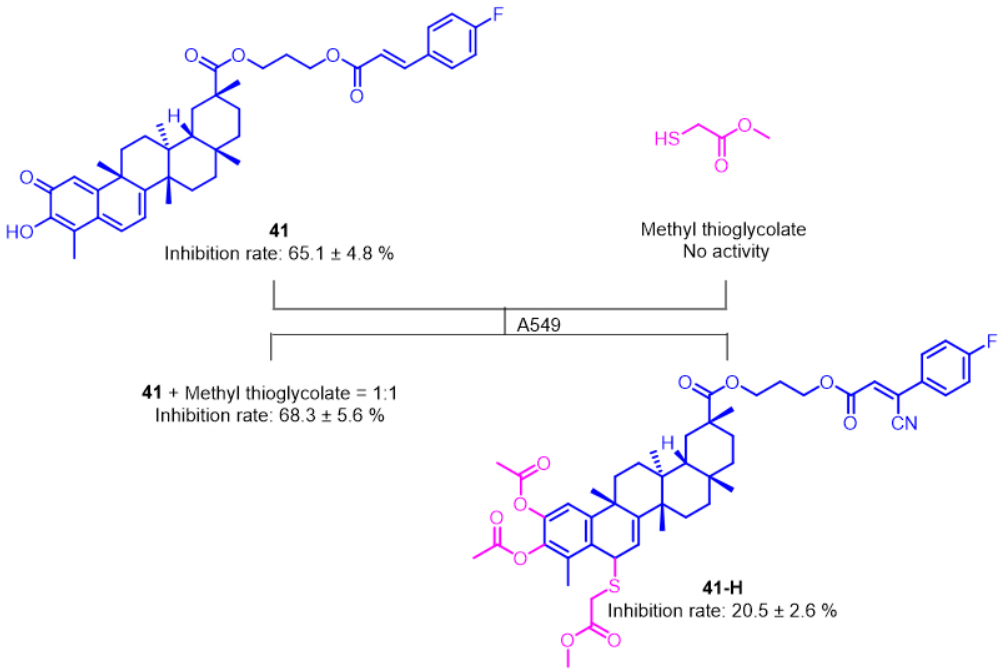

Anti-proliferative activity of 41-H in comparison with that of 41, methyl thioglycolate and the mixture of 41 and methyl thioglycolate in A549 cells.

211x141mm (96 x 96 DPI)

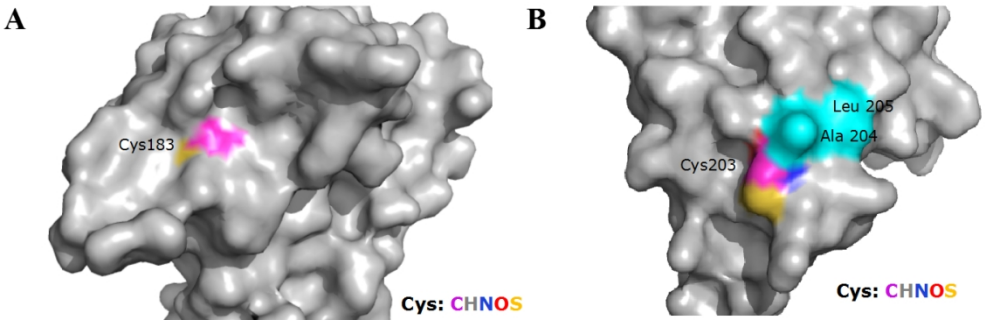

The structure of Cdc37M (PDB ID 2W0G). (A) The location of Cys183. (B) The location of Cys203.

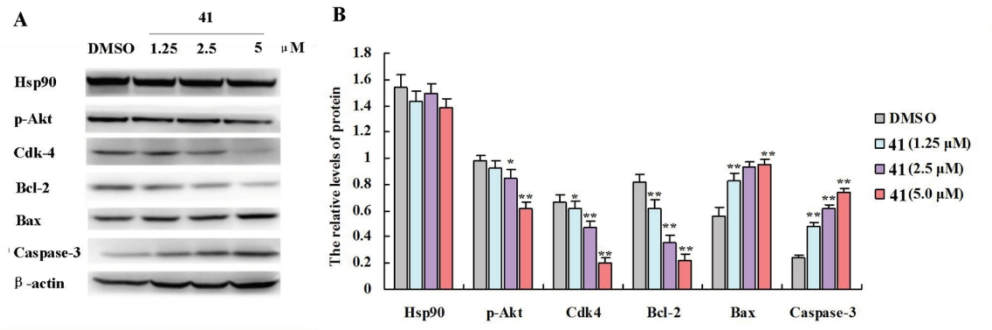

Effects of 41 on clients of Hsp90-Cdc37 and apoptosis-related proteins in A549 cells. A549 cells were treated with DMSO or 41 for 12 h, and the relative levels of Hsp90, p-AKT, Cdk4, Bcl-2, Bax and Caspase-3 expression were determined by Western blot assays using β-actin as a control. Data are representative images and expressed as the means ± SD of each group of cells from three separate experiments. (A) Western blot analysis of the relative levels of Hsp90, p-Akt, Cdk4, Bcl-2, Bax and Caspase-3 expression. (B) Quantitative analysis. *P < 0.05, **P < 0.01, vs the DMSO-treated control group.

150x52mm (300 x 300 DPI)

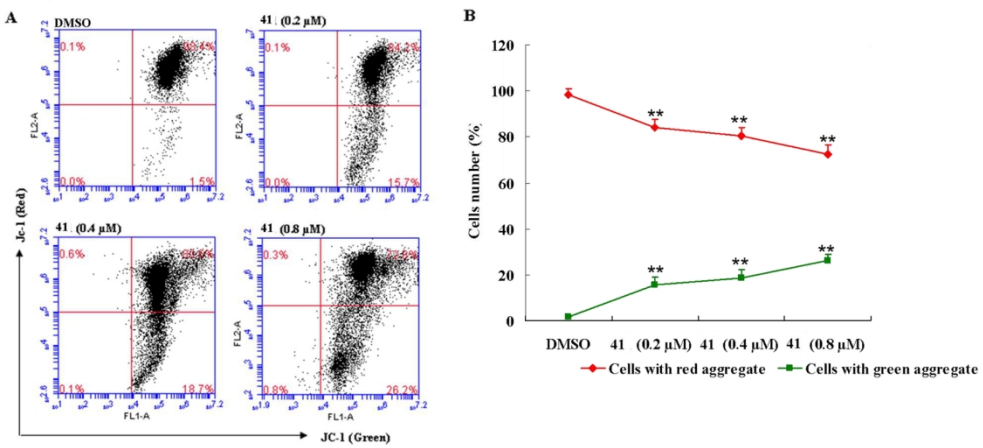

Effects on Δψm of 41 in A549 cells. A549 cells were treated with DMSO or 41 for 24 h and then analyzed by fluorescence microscopy and flow cytometry after JC-1 staining. (A) Flow cytometry analysis of A549 cells treated with DMSO and 41. (B) The quantification of cells (%) with red and green aggregates. The values are presented as mean ± SD (n = 3). **P < 0.01 vs. the DMSO group.

150x70mm (300 x 300 DPI)

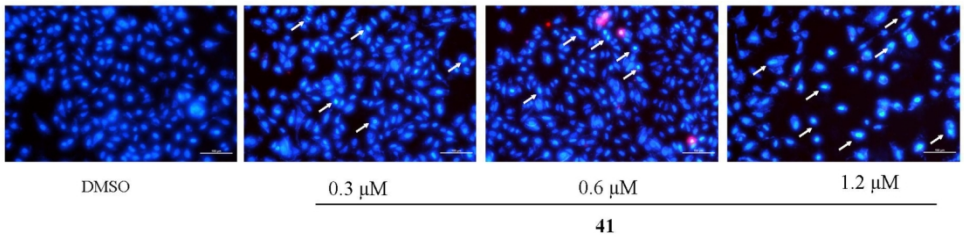

The morphological apoptosis induced by 41 in A549. A549 cells were treated with 41 or DMSO for 48 h. Fluorescence microscopy images of A549 cells stained by Hoechst 33342 and propidium iodide (PI). The apoptotic cells were stained by Hoechst 33342 in bright blue and the dead cells were stained by PI in red.

149x37mm (300 x 300 DPI)

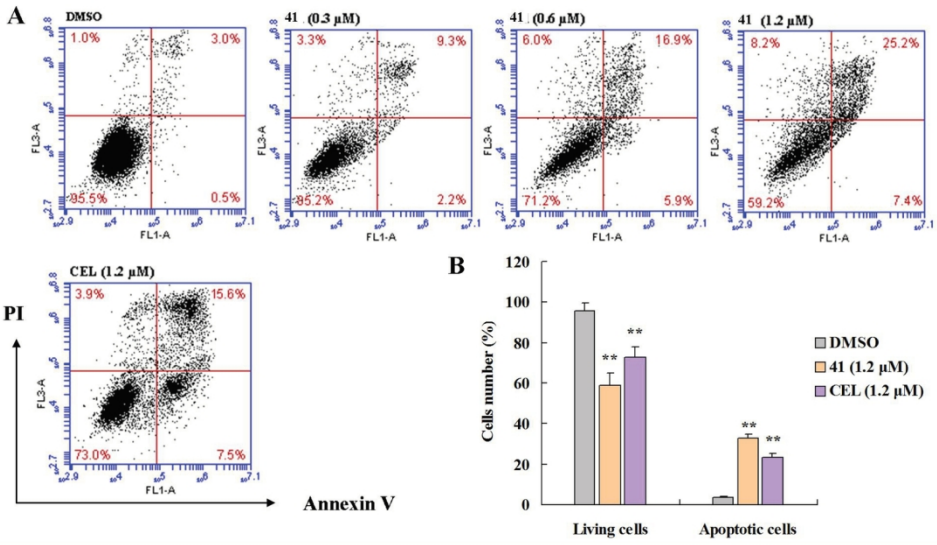

Apoptotic effects of 41 and CEL in A549 cells. Treatment with DMSO or 41 or CEL for 48 h, A549 cells were collected and stained with Annexin V/PI, followed by flow cytometric analysis. (A) Flow cytometry analysis of A549 cells treated with DMSO, 41 and CEL. (B) Representative histograms for the numbers of living cells and apoptotic cells (%). The values were presented as the mean ± SD (n = 3). **P < 0.05 vs. the DMSO group.

150x84mm (300 x 300 DPI)

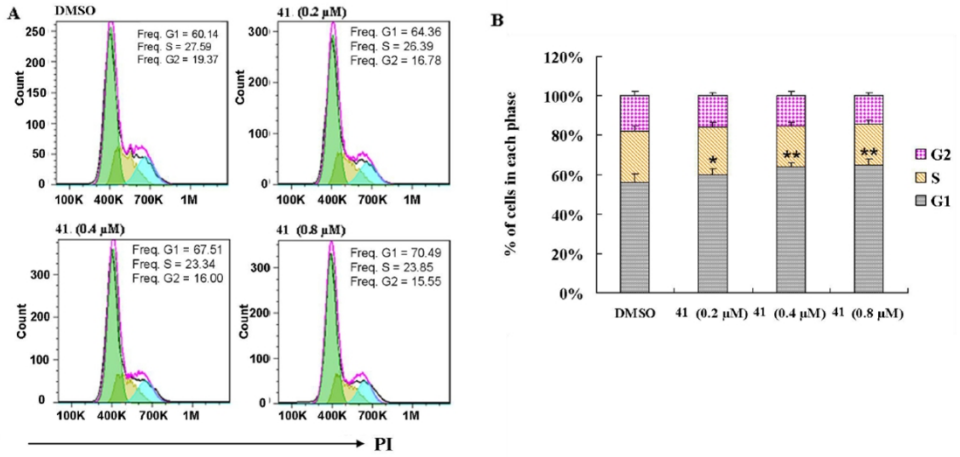

Effect of 41 on cell cycle progression of A549 cells. Treatment of A549 cells with DMSO and 41 (0.2, 0.4 and 0.8 μM) for 24 h, intracellular DNA was stained with PI. Cell cycle distribution was analyzed by flow cytometry. (A) Flow cytometry analysis of cell cycle distribution of 41 on A549. (B) The quantification of cells (%) in each cell phase. The values are presented as mean ± SD (n = 3). *P < 0.01, **P < 0.05 vs. the DMSO group.

150x74mm (223 x 223 DPI)

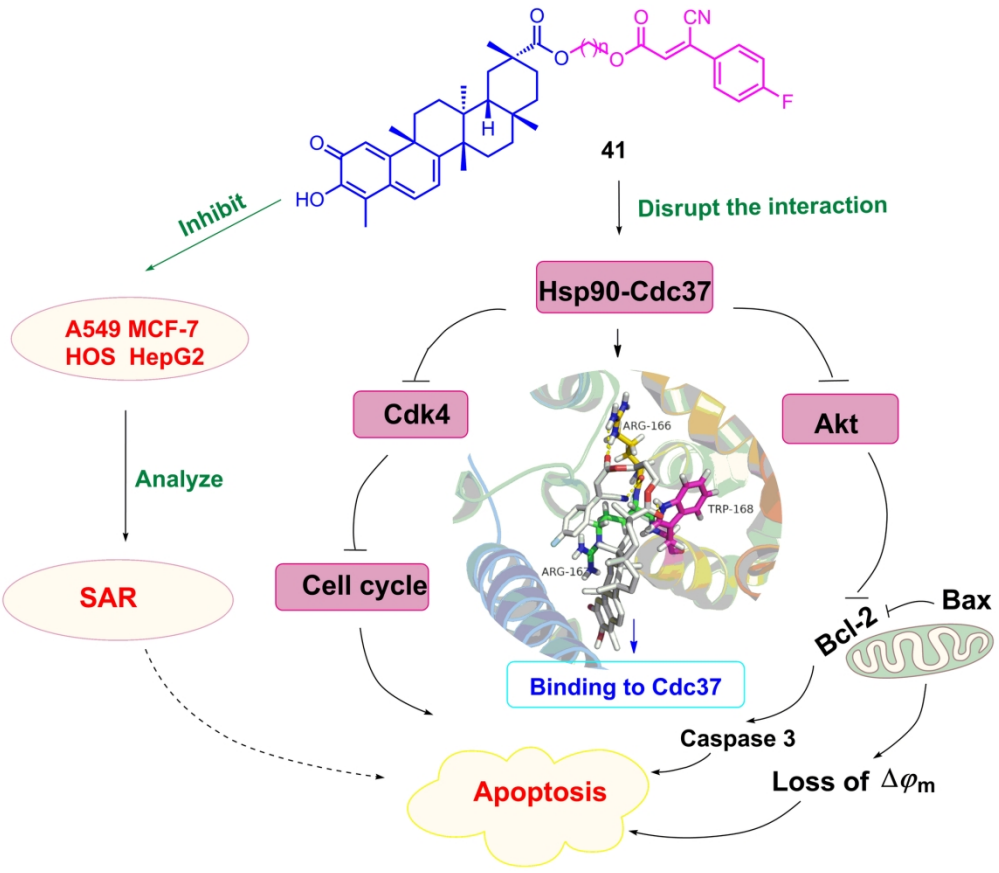

179x155mm (300 x 300 DPI)